

Chapter 6 Watching and analysis of various phenomena^{*}

6.1 Heavy rain

6.1.1 Procedure of image analysis

In heavy rain watching, use of satellite imagery is effective in terms of prompt report, observation frequency, wide-area uniform quality, and continuity. The image analysis making use of these merits is comprised of two analysis works on a synoptic scale and mesoscale, and proceeds in the following procedures (Figure 6-1-1):

[Analysis work on synoptic scale weather phenomena]

(1) Checking synoptic-scale weather phenomena on a weather chart

Check the synoptic-scale phenomena in Table 6-1-1 from the weather chart.

(2) Analyzing synoptic-scale clouds on the image

As shown in Table 6-1-1, analyze cloud and water vapor patterns on the image and find jet stream axes, troughs and other phenomena.

(3) Comparison synoptic-scale phenomena and weather chart. (Check of cloud analysis results against the synoptic weather fields on the weather chart.)

Comparison (1) and (2) above, and understand the synoptic-scale 3-dimensional structure of the atmosphere.

(4) Interpreting numerical weather forecast

If you find such a physical quantity in the numerical weather forecast that varies in good response to the behavior of bright and dark area or cloud area, keep track of the subsequent variations with time of that physical quantity and estimate the changes of weather distribution and 3-dimensional atmospheric structure.

(5) Estimating the changes of bright and dark regions and cloud area and watching the images

From the predicted distribution of weather phenomena and 3-dimensional atmospheric structure, predict the subsequent changes of the bright and dark regions and cloud area, and watch so as to catch indications of active convective cloud which have heavy rain and their occurrence, development and standstill.

^{*} 6.1 Kou Egami, 6.2 Nobutoshi Fuchita and Takeo Tanaka, 6.3 Nobutoshi Fuchita, 6.4 Kazufumi Suzuki and Shun'ichi Yamaguchi (Forecast Section, Forecast Department)

Table 6-1-1. Synoptic-scale phenomena as appearing in cloud and water vapor pattern and weather chart.

Synoptic-scale phenomena	Corresponding feature of cloud and water vapor pattern	Weather chart
Strong wind axis and upper air flow	Curvature and tangential directions of a boundary along a wind direction, Ci streak, and transverse line	200-hPa weather chart 300-hPa weather chart
Feature (intensity and movement) of middle-level trough and cold air	Change in cyclonic curvature and darkening of dark region, life cycle of upper vortex, and change in anticyclonic curvature of Ci streak and transverse line	500-hPa weather chart 500-hPa geopotential height and vorticity analysis chart
Water vapor distribution in middle troposphere	Darkening of dark region (atmospheric subsidence area in high and middle troposphere)	700-hPa weather chart
Ascending wind, temperature field and front in middle and low troposphere	Prosperity and decline of middle and low clouds, and degree of development of convective cloud	Ascending wind at 700 hPa 850-hPa temperature and wind analysis chart
Atmospheric wind (anticyclonic and cyclonic circulation), water vapor distribution and front in low troposphere	Prosperity and decline of low cloud area, and curvature and tangential directions of convective cloud line	850-hPa weather chart
Pressure pattern including highs, lows and fronts	Hook pattern in cloud area, life cycle of vortex in low levels, and tangential directions of convective cloud line	Surface weather chart

[Mesoscale weather phenomena analysis work]

(1) Checking mesoscale phenomena from variously observations.

Check the mesoscale phenomena in Table 6-1-2 from the radar, AMEDAS and surfaced observations.

(2) Mesoscale cloud analysis by imagery

Analyze the cloud patterns on the image and check instability areas and other phenomena as shown in Table 6-1-2.

(3) Comparison mesoscale phenomena and observations (check of cloud analysis results against the several kind of observation)

Comparison (1) and (2) above, and understand the meso-scale weather distribution and 3-dimensional atmospheric structure.

(4) Estimating the changes of a cloud area

Estimate (interpolate) the changes of a cloud area with the mesoscale phenomena while considering the changes of synoptic-scale phenomena, and watch so as to catch indications of active convective cloud which have heavy rain and their occurrence, development and standstill.

The points on image analysis are described below based on instances that bring about heavy rain (cold low, baiu front, anticyclonic marginal wind direction, and typhoon and front).

Table 6-1-2. Cloud patterns in mesoscale phenomena and observation data.

Mesoscale phenomena	Corresponding feature of cloud patterns	Observation data
Wind shear (convergence, divergence), and instability precipitation	Moving direction, life cycle and degree of development of cloud area	Radar, AMEDAS, surface observation
Low-level wind (wind shear, anticyclonic and cyclonic circulation)	Curvature and direction of convective cloud line, and position of low-level cloud vortex	

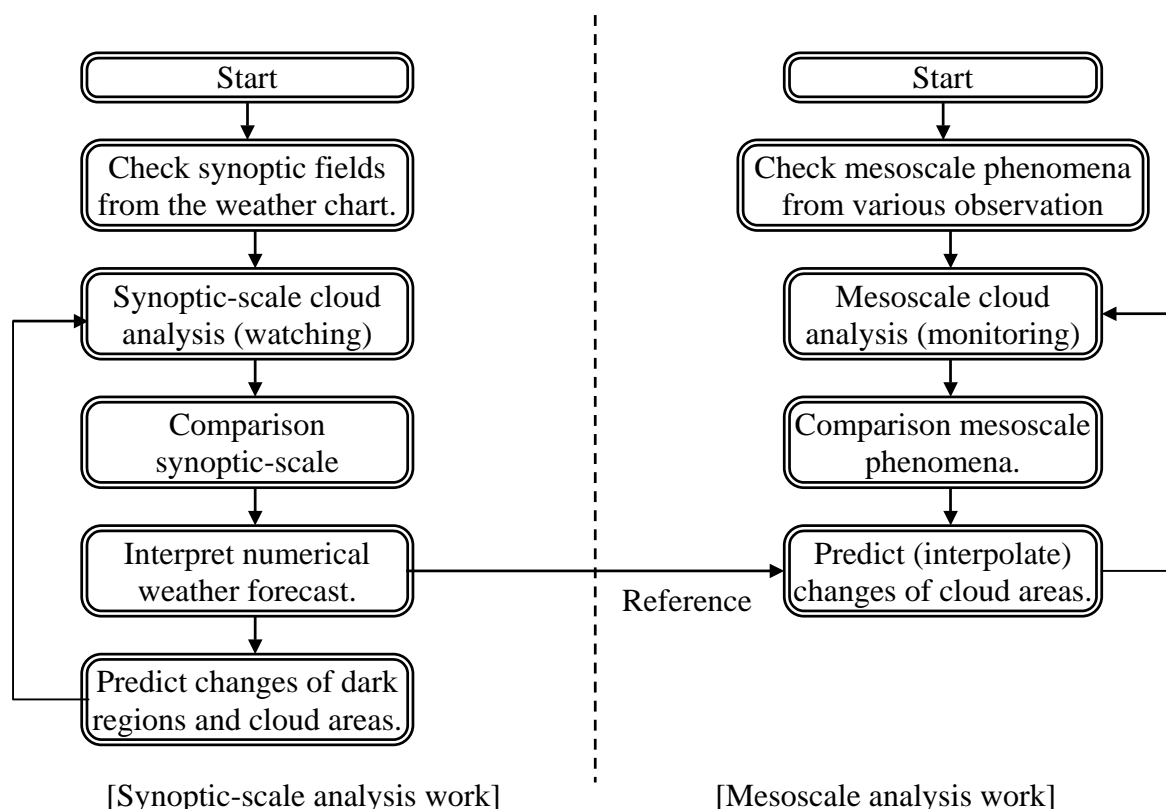


Figure 6-1-1. Image analysis work flow chart.

6.1.2 Instability around cold low

Major features of a cold low have cut-off of upper troposphere cold air (low), formation of a cold dome and subsidence of the tropopause. A surface low may develop just under a cold low or in front of cold low. For a cold low having cold air in the high levels, the convection becomes more active in front (east side) than behind (west side) in many cases (Obana, 1983). This is due to the following factor. At the east side of cold low, an intense ascending wind is formed in the low levels by a positive-vorticity advection in the middle levels and the instability is also intensified by the inflow of warm and humid air from the lower troposphere. This instability intensification causes the convection activity in front of the cold low looking in its moving direction.

Here, features of the image of a cold low are explained using a case where there was a water spout around the cold low.

(1) Feature of cold low and upper vortex

Because a vortex is visualized as a water vapor pattern on the water vapor image, it can be analyzed and kept track of as a upper vortex even if there is no cloud. In the water vapor image (Figure

6-1-2 a) of this case, a upper vortex can be analyzed near the point of wedge mark. This nearly corresponds to a cold core center (marked by X in Figure 6-1-2 a) at 500 hPa.

(2) Cloud area accompanying the surface low in front of a cold low

(Overview)

In the southeast quadrant of a cold low, a cloud area may occur corresponding to the (surface) low. In the warm section of this low, convective clouds develop in response to the inflow of warm and humid air by southerly wind.

(Points)

① Upper trough and cloud area exhibiting an anticyclonic curvature

In front of an upper trough, an intense ascending wind is formed by positive-vorticity advection, and a cloud area exhibiting an anticyclonic curvature tends to occur there.

In this case, an upper trough (B) extending toward south-southwest from around Cheju Island can be analyzed from the dark regions in the water vapor image (Figure 6-1-2 a) and the curvature of the Ci streak on the northern edge of the cloud area (A) in the infrared image (Figure 6-1-2 b). On the visible image (Figure 6-1-2 c), a thick cloud area (A) whose northern fringe shows an anticyclonic curvature spreads off San'in, and, on its western side, a low-level vortex (marked by a wedge) can be analyzed corresponding to a cyclonic circulation (marked by x) seen in the 850-hPa analysis chart.

② Active convective cloud area in warm sector

An active convective cloud area or cloud line corresponds to convergence area in low levels and a region of high equivalent potential temperature in many cases. The convergence in low levels may be judged by what tangential direction the convective cloud area or cloud line has and in which direction the convective cells comprising the cloud area or cloud line move.

On the infrared image and visible image (Figure 6-1-2 b, c) of this case, Cu (D) moves north-northeast toward an active convective cloud area (C). A cold front points to (C) and runs from southwest to northeast with Cb-Cb line (E). On this Cb-Cg line, individual convective cloud cells are moving northeast. From these, convergence in lower troposphere is suggested near (C). In the 850-hPa analysis chart (Figure 6-1-3) and the 700- and 850-hPa analysis chart (Figure 6-1-4), there are a convergence field of west-southwest and south-southwest winds, a region of high equivalent potential temperature higher than 324K, and an ascending wind area of intense warm advection around this (C).

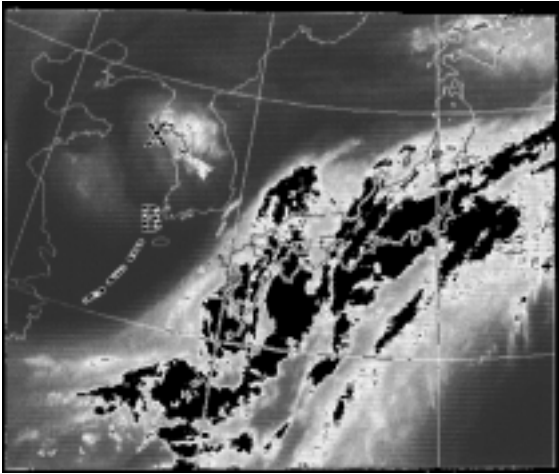


Figure 6-1-2 a.
Water vapor image at 00UTC, April 6, 1997
For symbols, refer to the text.

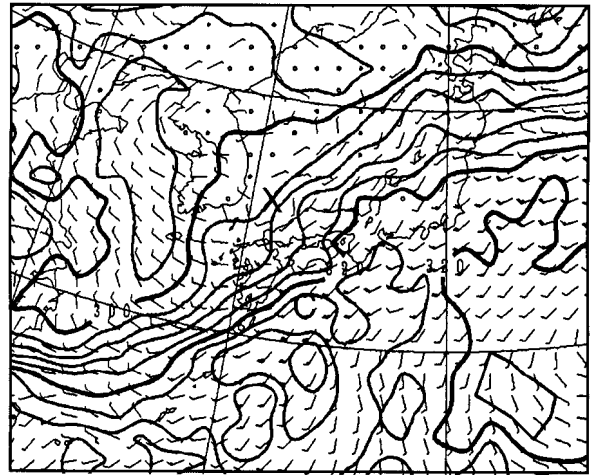


Figure 6-1-3. 850-hPa equivalent potential temperature and wind analysis chart at 00UTC, April 6, 1997.
For symbols, refer to the text.

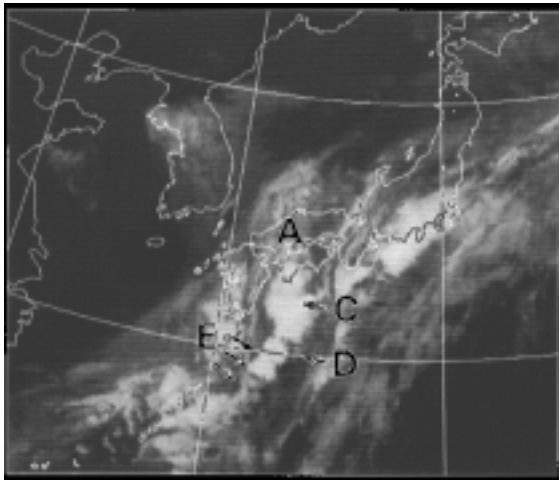


Figure 6-1-2 b.
Infrared image at 00UTC, April 6, 1997
For symbols, refer to the text.

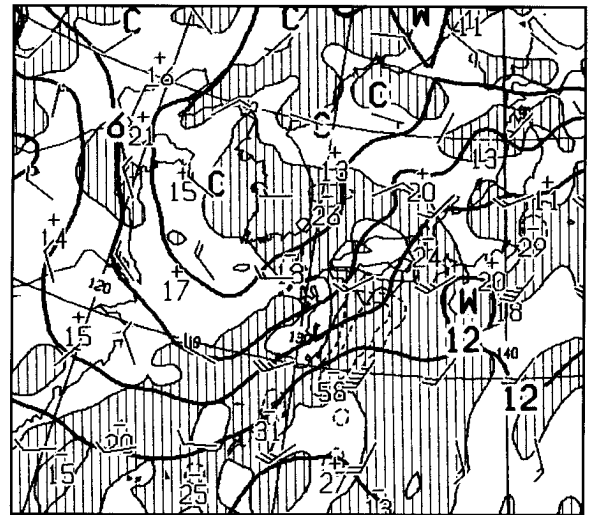


Figure 6-1-4. Analysis chart of ascending wind at 700 hPa and air temperature and wind at 850 hPa at 00UTC, April 6, 1997.

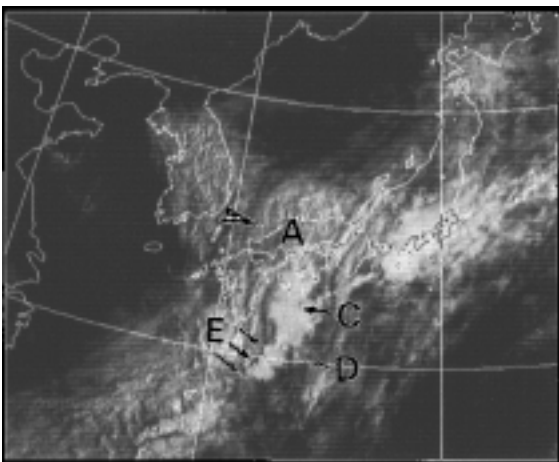


Figure 6-1-2 c.
Visible image at 00UTC, April 6, 1997
For symbols, refer to the text.

(3) Summary of surface low in front of cold low

From the viewpoint of heavy rain, features of imagery are summarized and represented as a schematic (Figure 6-1-5) with respect to a surface low in front of a cold low. The points are given below.

- When a surface low appears in the southeast quadrant of a cold low, the conversion in lower troposphere and inflow of warm and humid air from the south become distinct in the warm sector, and convective clouds are activated around there.

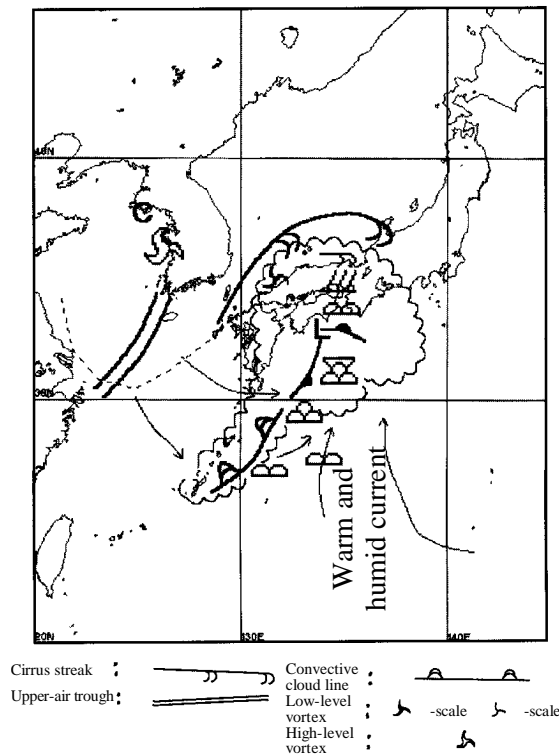


Figure 6-1-5. Schematic chart of low in front of cold low.

Broken line: Boundary between bright and dark regions in WV images

Arrow with thin shaft: Wind in lower troposphere

Corrugated closed curve: Cloudedge C: Cold core center

(4) Convective cloud area around cold low

(Overview)

When a low-level vortex becomes distinct due to an approach of a upper vortex accompanied by cold air, the low-level warm and humid air is transported to the front of the vortex. Therefore, convection is activated chiefly in front of the vortex. When the low-level warm and humid air flows to the north of the vortex, active convective clouds develop there.

(Points)

③ Dark region around cold low

On the water vapor image, a vortex in the bright sector is seen near the center of the upper vortex around which dark regions encircle. Dry areas, cold air and other air masses of low equivalent potential temperature appear in the dark regions. When they move to the upper levels of the troposphere whose lower level air has high equivalent potential temperature, they intensify the potential instability. Thus, the dark regions serve as a clue to prediction of convective activity.

In the water vapor image (Figure 6-1-6 a) of this example, an upper vortex corresponding to a cold low can be analyzed off the Kii Peninsula, and darkening (drying) of the dark region (F) accompanying a trough (as shown symbol B in Figure 6-1-2 a) is at south of Japan. In the infrared and visible images (Figures 6-1-6 b and c), a Cb-Cg line (G) corresponding to a cold front has become distinct along the edge of (F). This (G) extends along the area of high equivalent potential temperature (320K or higher) in the 850-hPa analysis chart (Figure 6-1-7).

④ Occurrence of low-level vortex

In the infrared and visible images (Figures 6-1-6 b and c) of this example, a low-level vortex (marked by X) becomes distinct at the place pointed by a Cu line (H) having a cyclonic curvature, and Cg (I) has occurred in front of the vortex. This place corresponds to the portion (I) where the equivalent potential temperature gets into the inland in convex form in the 850-hPa analysis chart (Figure 6-1-7). In the infrared image (Figure 6-1-8) nine hours after, a low-level vortex (marked by X) was analyzed almost directly below a upper vortex lying around the Boso Peninsula, and a spout was observed at Yokohama in the vicinity of the vortex.

It may happen that the active convective clouds expand to the north of the low-level vortex. In the infrared image at 12UTC, June 30, 1999 (Figure 6-1-9), an active convective cloud (J) is seen on the north of the low-level vortex (marked by X). In the 850-hPa analysis chart (Figure 6-1-10) at the same time of day, warm and humid air (equivalent potential temperature of 328K or over) flows in off Akita.

(5) Summary

From the viewpoint of heavy rain, features of imagery are summarized and represented as a schematic (Figure 6-1-11) with respect to a cold low. The points are given below.

- Convective clouds become active where the dark regions around a cold low are in contact with low-level warm and humid air.
- When a low-level vortex becomes distinct near a cold low, convective clouds become active chiefly in front of the low-level vortex.

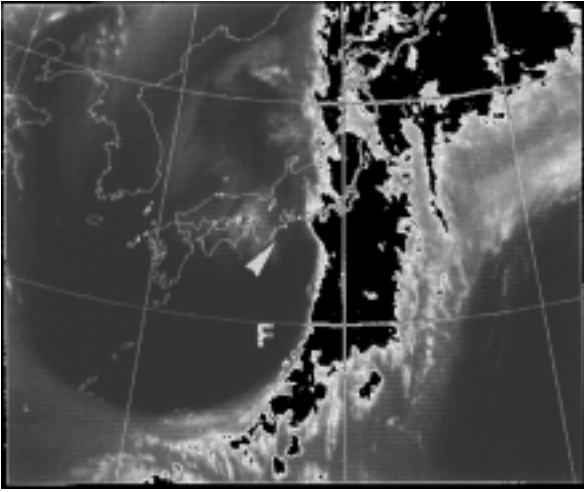


Figure 6-1-6 a.
Water vapor image at 00UTC, April 7, 1997
For symbols, refer to the text.

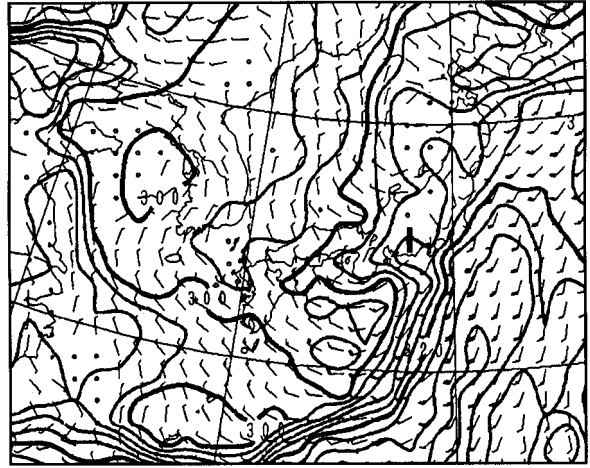


Figure 6-1-7.
850-hPa equivalent potential temperature and wind
analysis chart at 00UTC, April 7, 1997.

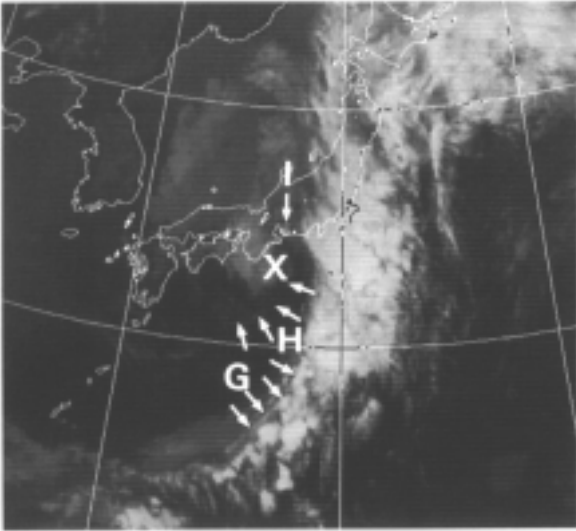


Figure 6-1-6 b.
Infrared image at 00UTC, April 7, 1997
For symbols, refer to the text.

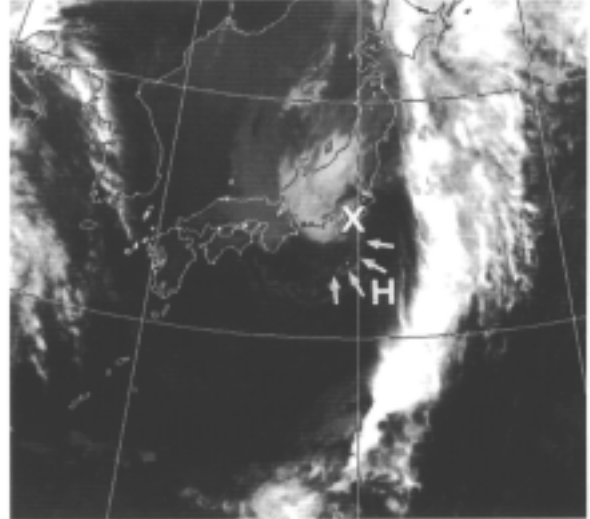


Figure 6-1-8. Infrared image at 09UTC, April 7,
1997 (gradation enhanced for low levels). For
symbols, refer to the text.

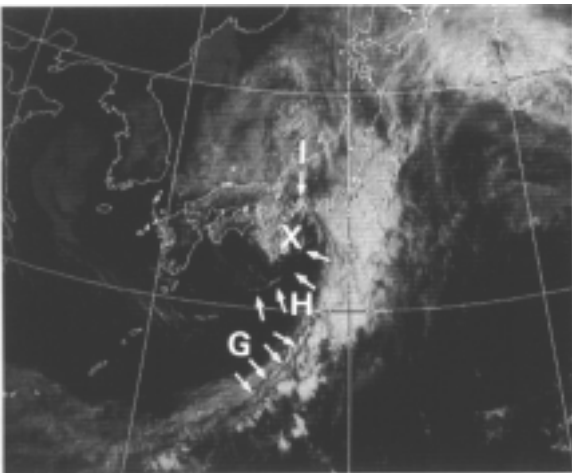


Figure 6-1-6 c.
Visible image at 00UTC, April 7, 1997
For symbols, refer to the text.

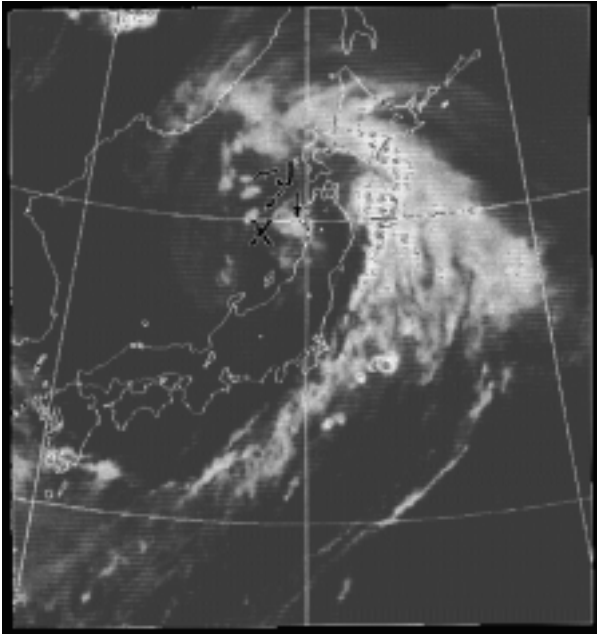


Figure 6-1-9.
Infrared image at 12UTC, June 30, 1999
For symbols, refer to the text.

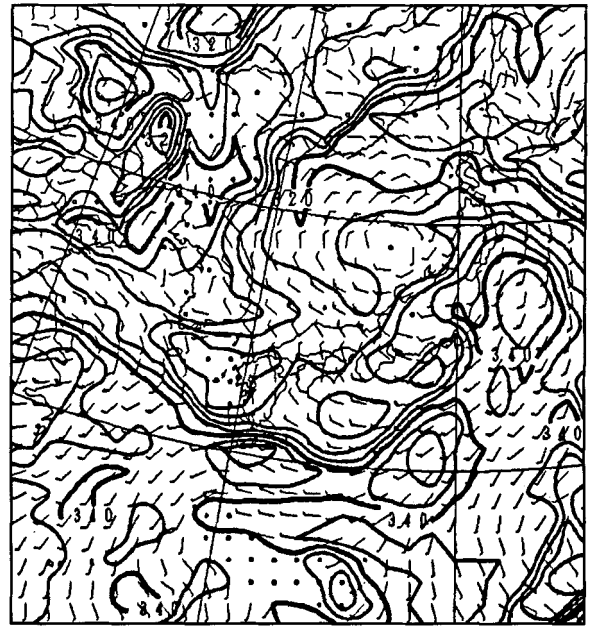


Figure 6-1-10.
850-hPa equivalent potential temperature and wind
analysis chart at 12UTC, June 30, 1999.

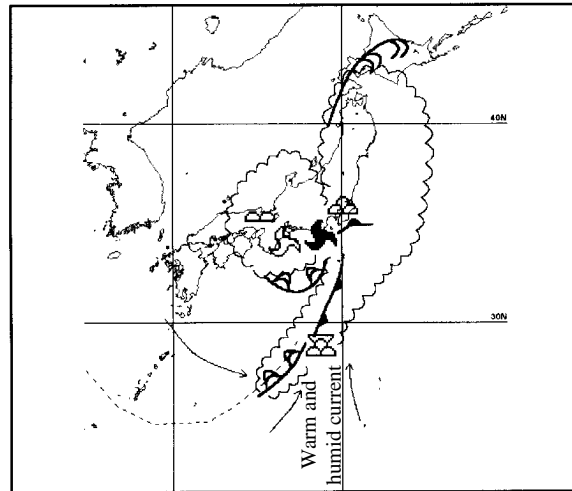


Figure 6-1-11. Schematic with respect to a cold low
Same symbols as in Figure 6-1-5.

6.1.3 Baiu front activated by a trough or warm and humid air

Major features of a baiu front include a small temperature gradient horizontally but a large water vapor gradient, the presence of a low-level jet stream, and an intense inflow of warm and humid air (moist tongue). On the satellite image, a baiu front is seen as a latitudinally running cloud band. Information representing frontal activities is available in plenty from the satellite image, including the cloud band's width, length and meridional movements, which change from day to day, and the life cycle and movements of a convective cloud area in the cloud band and a convective cloud intruding in the cloud band. Wide-area data can be acquired from the satellite image in a nearly real-time basis, so the satellite image is important for watching heavy rain due to a baiu front.

Here, features of the image with respect to a baiu front are explained using an example of a baiu front (June 21 to 22, 1997) which was influenced by an upper trough and warm and humid air at the same time.

(1) Cloud band associated with front and convective cloud area in warm sector

(Overview)

When an upper trough approaches a cloud band associated with a front, a cloud area having an anticyclonic curvature on the northern edge begins to form. On the warm air side, convective clouds move north along the periphery of a subtropical high and toward the cloud band. In the convective clouds of warm air side, developed convective cloud lines may be seen.

(Points)

① Upper vortex associated with trough and cloud area exhibiting anticyclonic curvature

When an upper trough approaches a cloud band, a cloud area begins to form in the cloud band while exhibiting an anticyclonic curvature and increasing in thickness. This is the same feature as seen at the time of occurrence and development of a low.

In the water vapor image (Figure 6-1-12 a) of this example, a trough axis (indicated by a broken line) can be analyzed as extending from the upper vortex (A) around the Korean Peninsula. This corresponds to the area of maximum positive vorticity (A') in the 500-hPa analysis chart (Figure 6-1-13). On the infrared and visible images (Figures 6-1-12 b and c), the cloud band is increasing in thickness over the western Japan (B) in front of the trough. The cloud band has expanded on the northern edge in bulge form.

② Area of active convection near front and in warm sector

As described in Point ② in Section 6.1.2 "Cold Low", an active convective cloud area or cloud line occurs associated with a low-level convergence and an area of high equivalent potential temperature in many cases.

In the infrared and visible images (Figures 6-1-12 b and c) of this example, a convective cloud containing Cb is seen in the cloud band from the lower basin of the Changjiang to the East China Sea (C) and over the ocean waters (D) east of Taiwan on the warm side. The convective cloud (E) containing Cg over the East China Sea moves northeast, and an active cloud cluster (F) is seen over the ocean waters southwest of Kyushu. According to the 850-hPa analysis chart (Figure 6-1-14), the area around (C) corresponds to an area of distinct low-level convergence and of high equivalent potential temperatures of 344K or higher. The areas (D) and (E) are also the area of high equivalent potential temperatures of 344K or higher, and they move northeast by the marginal wind of a Pacific high.

The heavy rain potential is usually high in an area of high equivalent potential temperature in the lower troposphere. However, Ninomiya and Yamazaki (1979) points out a still higher heavy rain potential in a region of a large amount of warm and humid advection in the area of high equivalent potential temperature in the low levels. In Figure 6-1-14, the horizontal gradient of equivalent potential temperature is larger around (C) and (F) than around (D) and (E). Of these, (F) lies in the region of largest warm and humid advection in particular because the wind direction is perpendicular to the isograms of equivalent potential temperature there.

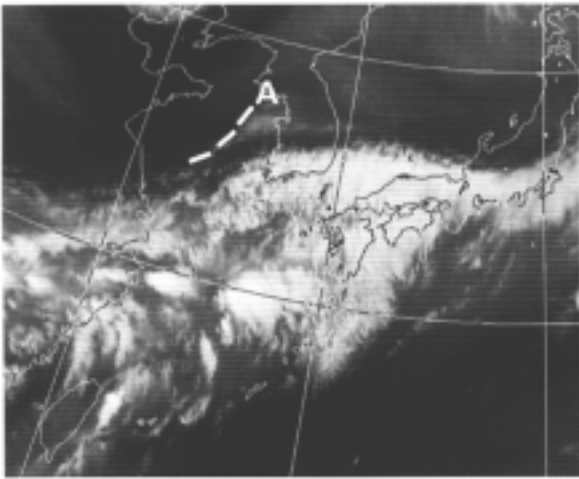


Figure 6-1-12 a.
Water vapor image at 00UTC, June 22, 1997
For symbols, refer to the text.

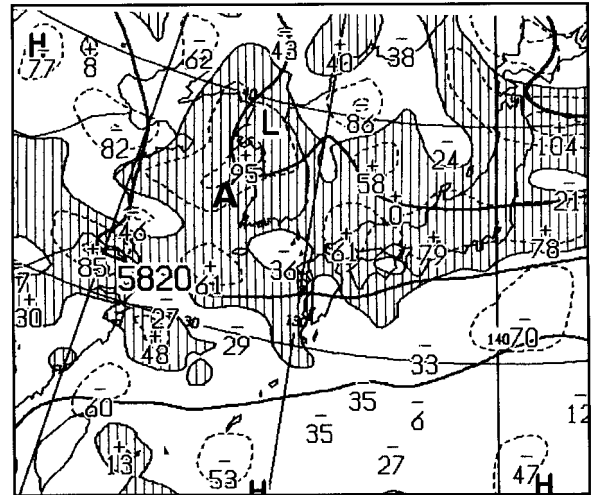


Figure 6-1-13. 500-hPa geopotential height and vorticity analysis chart at 00UTC, June 22, 1997
For symbols, refer to the text.

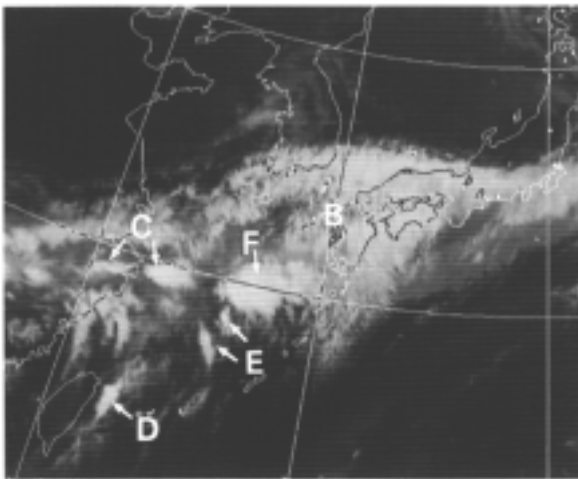


Figure 6-1-12 b.
Infrared image at 00UTC, June 22, 1997
For symbols, refer to the text.

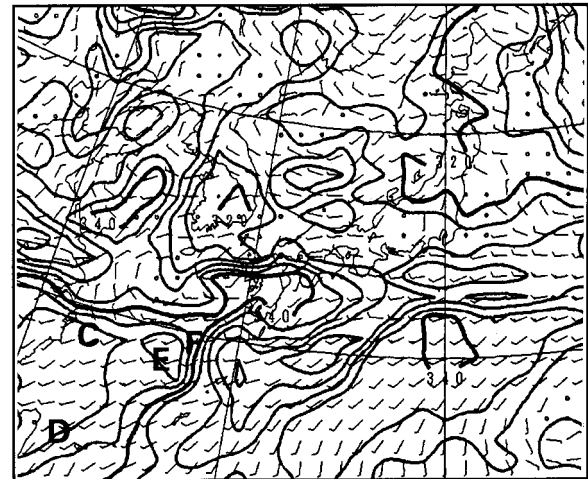


Figure 6-1-14.
850-hPa equivalent potential temperature and wind analysis chart at 00UTC, June 22, 1997
For symbols, refer to the text.

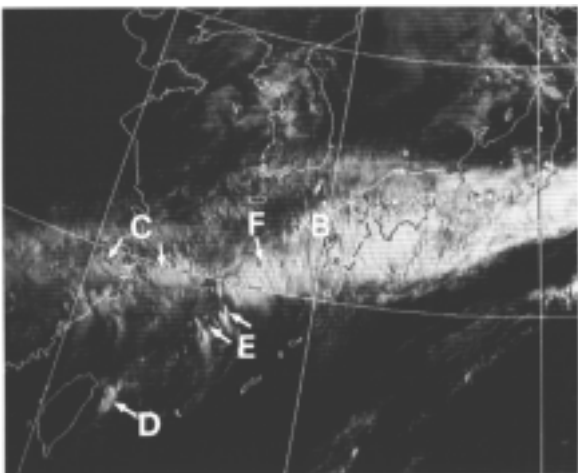


Figure 6-1-12 c.
Visible image at 00UTC, June 22, 1997
For symbols, refer to the text.

(2) Summary

From the viewpoint of heavy rain, features of imagery are summarized and represented as a schematic (Figure 6-1-15) with respect to a baiu front. The points are listed below.

- When an upper trough approaches a cloud band associated with a front, a thick cloud area having an anticyclonic curvature is formed in that cloud band.
- In a cloud band associated with a front, convection becomes active where low-level convergence is distinct.
- On the warm side, convection becomes active due to the marginal wind of a Pacific high in an area of high equivalent potential temperature in the lower troposphere.
- On the southern edge of the cloud band, convection becomes active particularly where warm and humid advection is large due to the marginal wind.

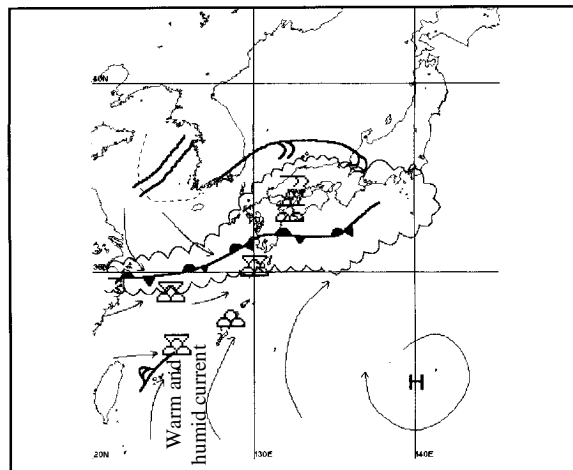


Figure 6-1-15. Schematic with respect to baiu front
Same symbols as in Figure 6-1-5.

6.1.4 Front activated by marginal wind of high or typhoon

When the marginal wind of a subtropical high or a warm and humid air mass of a tropical disturbance moves north, frontal activity is frequently activated. It is possible on the water vapor image to detect the axis of the subtropical high and areas of atmospheric subsidence. On the infrared and visible images, an area of low-level convergence and the like can be kept track of from the movements of the cloud band associated with the front and the convective clouds moving along the margin of the high. These serve as a clue to predicting heavy rain. If a convective cloud area or cloud line accompanying a typhoon flows in a cloud band associated with a front, heavy rain is more probable.

Features of the image are explained here using an example of activation of a front by approach of a marginal wind and typhoon (August 26 to 31, 1998, surface weather charts shown in Figures 6-1-16 a and b).

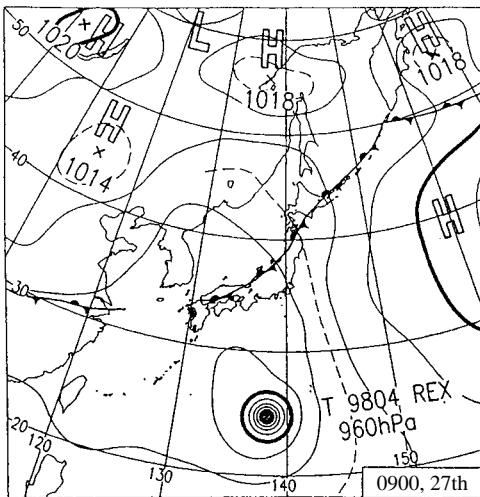


Figure 6-1-16 a. Surface weather chart at 00UTC, August 27, 1998.

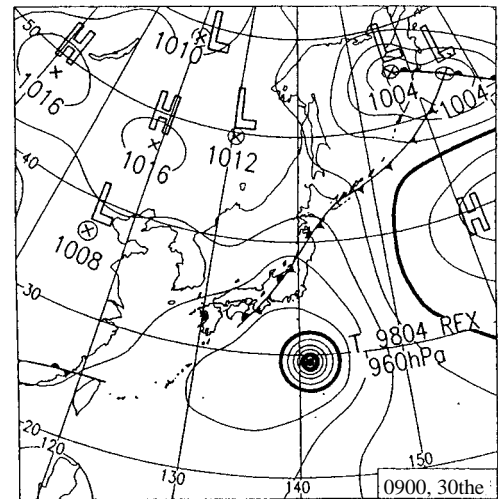


Figure 6-1-16 b. Surface weather chart at 00UTC, August 30, 1998.

(1) Cloud band associated with front and convective cloud area of marginal wind

(Overview)

When a warm and humid air mass comes flowing around the margin of a subtropical high into a cloud band associated with a front, convective clouds develop on the southern edge of the cloud band. In the cloud band, active convective cloud areas rendered stationary under the influence of the topography or the like are also seen.

(Points)

① Convective cloud area or cloud line associated with marginal wind

By analysis of the movements of convective cloud areas associated with a marginal wind, information can be extracted “about the conditions of convective activity”, “about the axis of a subtropical high from the curvature of a cloud line” and “about the convergence in the lower troposphere from the movements of a cloud line toward a cloud band associated with a front” respectively.

In the water vapor and infrared images (Figures 6-1-17 a and b) of this example, there is a subtropical high over the ocean waters east of Japan. From the curvature of the western edge (A) of the dark region associated with the subtropical high and a convective cloud line (B) having an anticyclonic curvature, the axis of the high can be estimated near 37 to 40° north. There is an active convective cloud (D) on the southern edge of a cloud band (C), and the advancing direction of (B) intersects with the cloud band at D. It can be seen on the 850-hPa analysis chart (Figure 6-1-18) that the cloud line (B) is associated with the marginal wind of the subtropical high. The area around (D) corresponds to an area of high equivalent potential temperature of 340K or higher.

② Topographically affected convective cloud area

Some of the active convective cloud areas may grow depending on the topography if the upslide wind on a slope is intensified. If an environment favorable for the growth of such a cloud area lasts, the cloud area may appear stationary as a whole whereas its individual cells follow their life cycle in succession. Whether the cloud area moves or is stationary is important for prediction of

heavy rain.

In the infrared image (Figure 6-1-17 b) of this example, an active cloud area (E) near the border between Tochigi and Fukushima Prefectures is estimated to become stationary under the influence of the topography. It alternated growth and decay while it was stationary for several hours. According to the 850-hPa analysis chart (Figure 6-1-18), the wind direction at 850 hPa is the south near (E). It seems that this was associated with the forced ascending by the topography near the border between Tochigi and Fukushima Prefectures (Tokyo District Meteorological Observatory, Tokyo Meteorological Observatory Investigation Data No. 141).

For details of the topographical effect in this example, refer to the Meteorological Agency Technical Report (will be issued in March 2000).

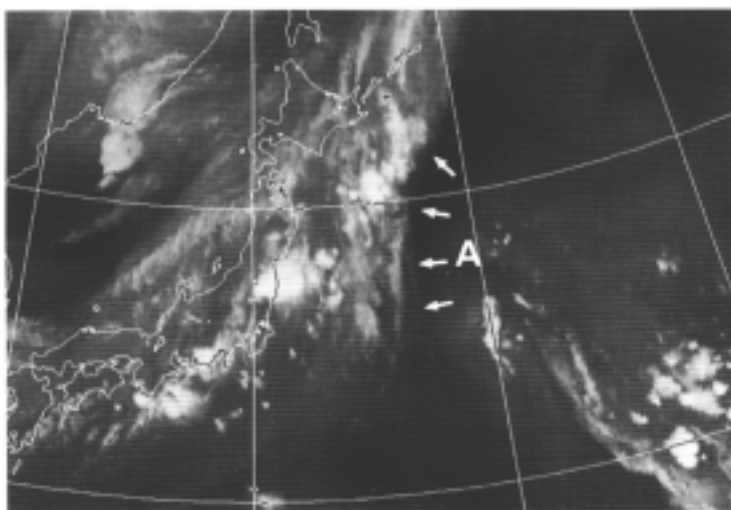


Figure 6-1-17 a. Water vapor image at 21UTC, August 26, 1998
Symbols: Refer to the text.

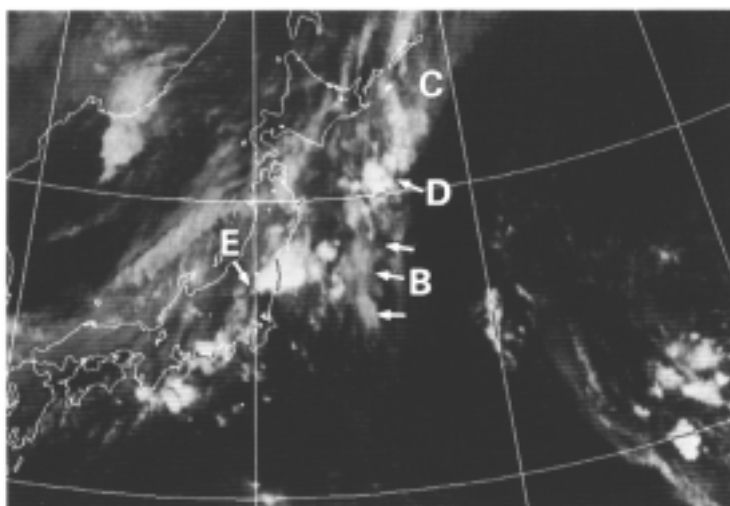


Figure 6-1-17 b. Infrared image at 21UTC, August 26, 1998
Symbols: Refer to the text.

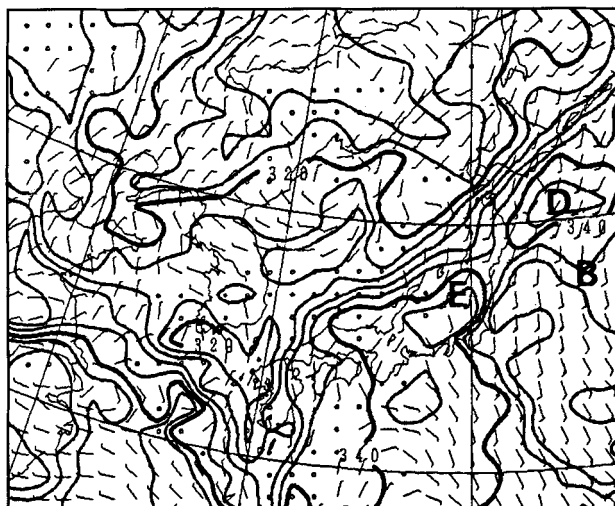


Figure 6-1-18. 850-hPa equivalent potential temperature and wind analysis chart at 00UTC, August 27, 1998. Symbols: Refer to the text.

(2) Cloud band associated with a front and cloud area accompanying a typhoon

(Overview)

When warm and humid air flows into a front-associated cloud band from a typhoon, the convective clouds on the southern edge of the cloud band are activated.

(Points)

- ③ In contrast to a cloud line along a marginal wind which exhibits an anticyclonic curvature, a cloud line accompanying a typhoon shows a cyclonic curvature.

In the infrared and visible images (Figures 6-1-19 a and b) of this example, a convective cloud line (F) is seen in the northeast quadrant of a typhoon, and it differs in curvature from the cloud line (G) along the marginal wind just on the east. At southern Kanto District toward which this cloud line (F) advances, convection is active on the southern edge (H) of the cloud band. In the 850-hPa analysis chart (Figure 6-1-20), an inflow of warm and humid air (equivalent potential temperatures of 344K or higher) is seen from the typhoon to around (H) where convection is active.

(3) Summary

From the viewpoint of heavy rain, features of imagery are summarized and represented as a schematic (Figure 6-1-21) with respect to an anticyclonic marginal wind, typhoon and front. The points are listed below.

- The convective cloud line along a marginal wind of a subtropical high exhibits an anticyclonic curvature, and convection is activated on the southern edge of a front-associated cloud band into which warm and humid air flows.
- The convective cloud line accompanying a typhoon exhibits a cyclonic curvature, and convection is activated on the southern edge of a cloud band into which warm and humid air flows.

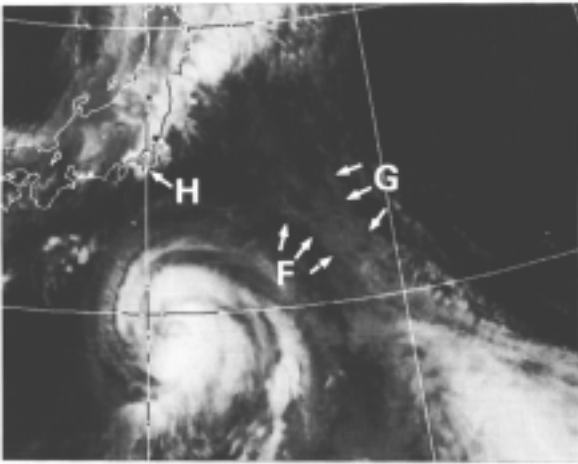


Figure 6-1-19 a.
Infrared image at 00UTC, August 30, 1998
Symbols: Refer to the text.

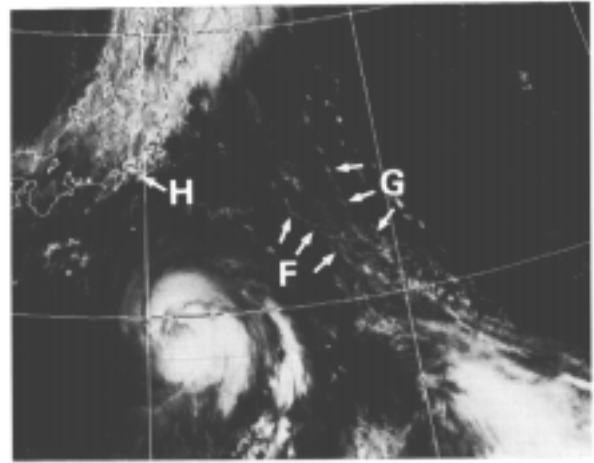


Figure 6-1-19 b.
Visible image at 00UTC, August 30, 1998
Symbols: Refer to the text.

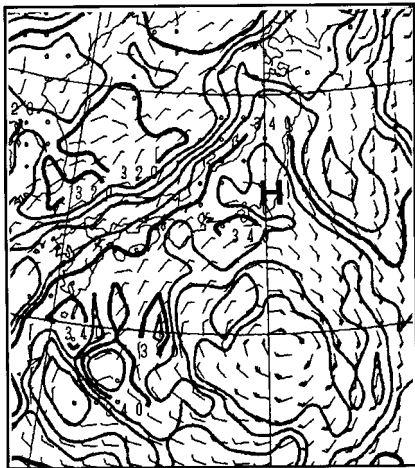


Figure 6-1-20.
850-hPa equivalent potential temperature and wind
analysis chart at 00UTC, August 30, 1998.
Symbols: Refer to the text.

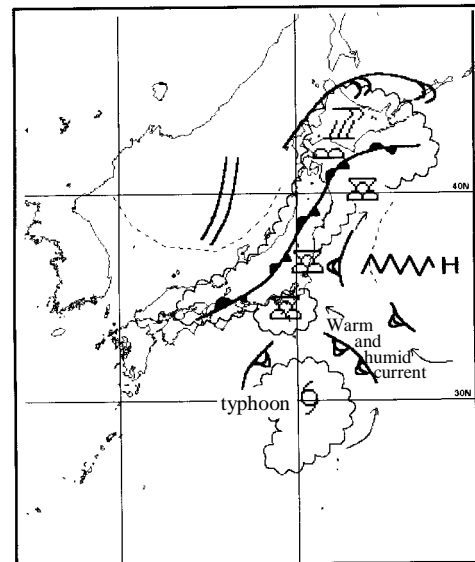


Figure 6-1-21.
Schematic with respect to front
Serrated line: Ridge.
Others are the same as in Figure 6-1-5.

6.2 Heavy snow

6.2.1 Convective cloud belt

When in the hibernal pressure pattern, a convective cloud belt (see Section 3.19) comprised of active cumulus or cumulonimbus is sometimes seen in the western Sea of Japan. The convective cloud belt is closely related to heavy snow on the Sea of Japan coast, and the Hokuriku line of discontinuity observed at heavy snow lies on the southern edge of the convective cloud belt.

When a convective cloud belt appears, the upper levels form a synoptic-scale trough around Japan in many cases. A low-level vortex is formed in the convective cloud belt, and it brings about heavy snow in many cases when it lands. The low-level vortex corresponds to a mesoscale cyclone, which may develop into a synoptic-scale cyclone. There is a report (Naito, 1992) saying,

“the meridional oscillation covering an entire convective cloud belt is associated with the passage of a meso-scale trough (at 500 hPa), and the low-level vortex forming on the convective cloud belt corresponds to a thermal trough (cold core at 700 hPa) behind this trough”.

Described below is the developmental process of a convective cloud belt from January 23 to 24, 1998.

(1) Developing stage of convective cloud belt

At 06UTC, January 23, low-level vortices (A and B) appeared on a convective cloud line, and the convective cloud line changed in direction near the low-level vortex (A). That is, the portion of the convective cloud line east of the low-level vortex (A) extends to the east and points to the Noto Peninsula, and the western portion extends to the southeast. The cloud top height of the convective cloud line is not high, or at around the height of cumulus (Figure 6-2-1).

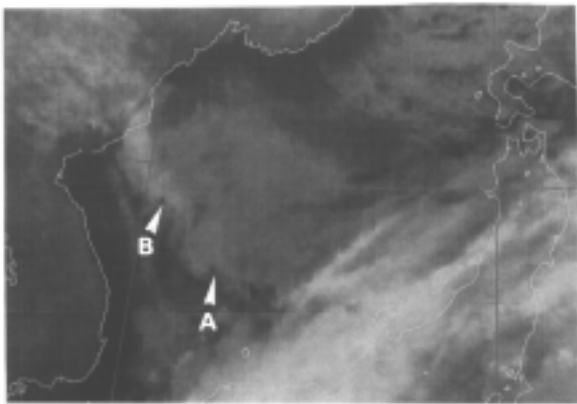


Figure 6-2-1 a. IR image of convective cloud belt at developing stage at 06UTC, January 23, 1998. Symbols: Refer to the text.

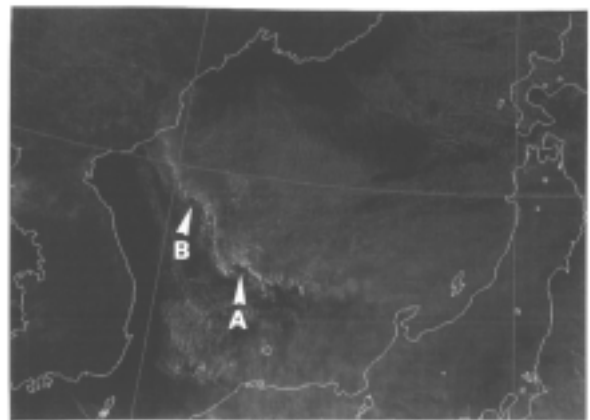


Figure 6-2-1 b. VIS image of convective cloud belt at developing stage at 06UTC, January 23, 1998. Symbols: Refer to the text.

At 12UTC, 23rd, the low-level vortex (A) on the convective cloud belt developed and was accompanied by Cg around, and a surface low (not shown) was analyzed. The area in front of this low-level vortex (A) and from the northern Noto Peninsula to around Niigata Prefecture is covered by a cumulus area. The low-level vortex (B) also began to develop and was accompanied with Cg around. Behind this, or off Wonsan, a new cloud area (C) comprised of Cg is appearing. At this time, a trough at 500 hPa lies around the Yellow Sea, and cold air at -30° at 700 hPa in the northern Korean Peninsula (Figure 6-2-2).

At 18UTC, 23rd, or additional 6 hours after, the low-level vortex (A) had moved east and lay around the Noto Peninsula. The cloud top height began to lower near the low-level vortex. The convective cloud area in front of the low-level vortex had moved east-northeast, and it landed the Sea of Japan coast of Tohoku District and became indistinct. The low-level vortex (B), which had been developing 6 hours before, decayed and became indistinct at this time. Small-scale, low-level vortices on a convective cloud belt have the feature of alternating growth and decay for a short time. The cloud area (C), which had appeared 6 hours before, further elongated to the southeast and became a convective cloud belt. The cloud top height increased, and Cg and Cb were seen. Across the convective cloud belt, the difference in direction of the cloud streets has become distinct (north to south on the north, and east to west on the south) (Figure 6-2-3).

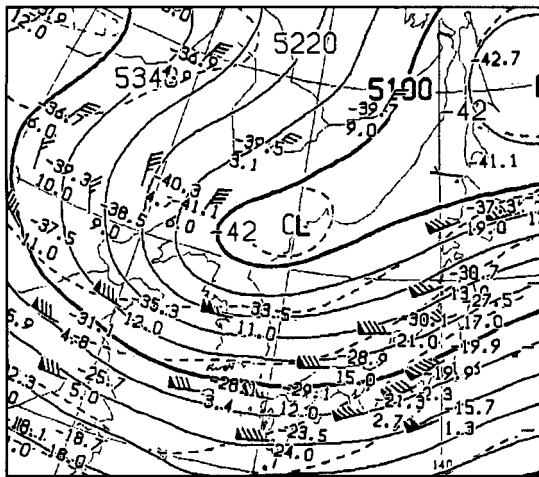


Figure 6-2-2 a.
500-hPa weather chart at 12UTC, January 23, 1998

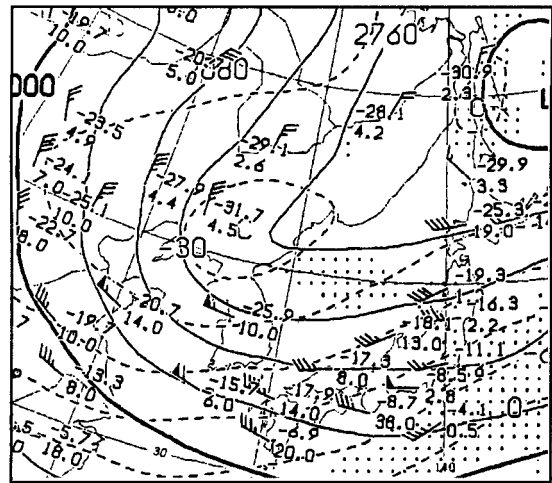


Figure 6-2-2 b.
700-hPa weather chart at 12UTC, January 23, 1998

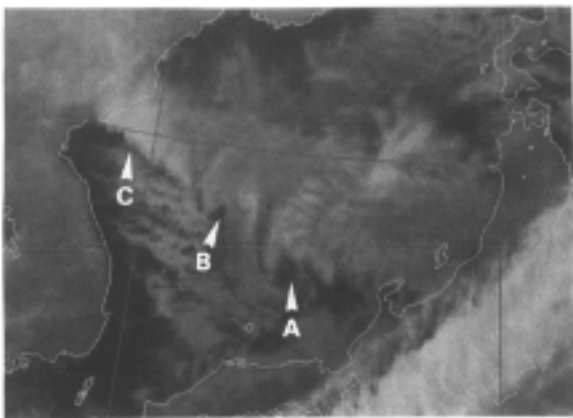


Figure 6-2-2 c. IR image of convective cloud belt at developing stage at 12UTC, January 23, 1998.
Symbols: Refer to the text.

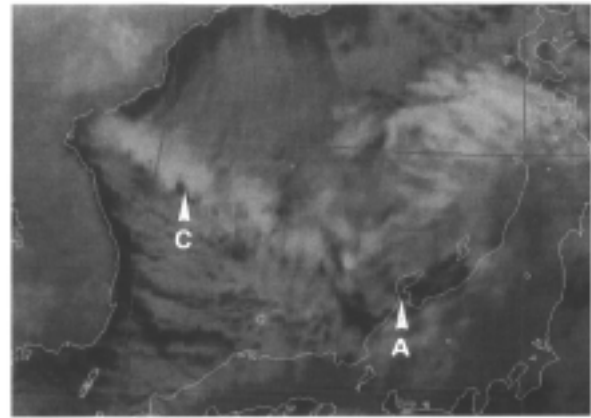


Figure 6-2-3. IR image of convective cloud belt at developing stage at 18UTC, January 23, 1998.
Symbols: Refer to the text.

(2) Mature stage

At 00UTC, 24th, the low-level vortex (A) landed around Niigata Prefecture and dissipated. The convective cloud belt in the central and western Sea of Japan began to move south gradually and had come to have an east-west direction. The low-level vortex (B) dissipated, but its phase landed around Toyama Prefecture where it brought a new snowfall of 20 to 30 cm for about 10 hours. There was also a snowfall of 40 to 60 cm in the western mountainous regions of Niigata Prefecture. A new low-level vortex (D) appeared on the convective cloud belt. The top height of the convective cloud belt remained high and showed no change, and the Cg and Cb cloud lasted. At this time, a trough at 500 hPa lay over the Sea of Japan and a thermal trough at -24°C at 700 hPa over the Yellow Sea and western Sea of Japan (Figure 6-2-4).

Additional 6 hours after, or 06UTC, 24th, the convective cloud belt began to move south further and reached off San'in. The cloud top height showed no change and remains high. The low-level vortex (D) reached off Ishikawa Prefecture and was accompanied with Cg and Cb clouds around (Figure 6-2-5).

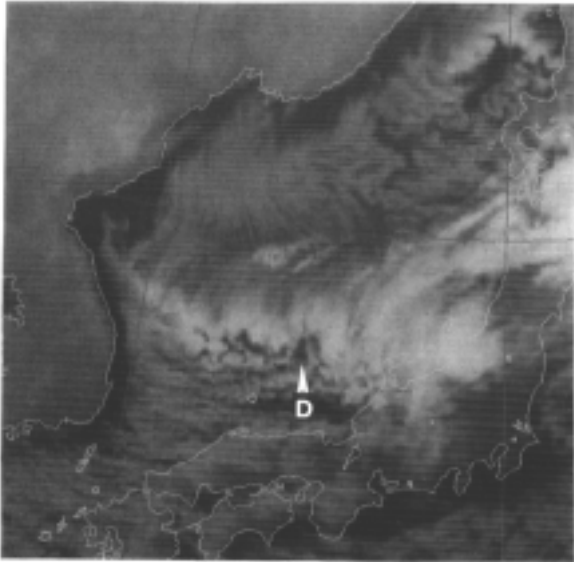


Figure 6-2-4 a. IR image at maturity at 00UTC, January 24, 1998.
Symbols: Refer to the text.

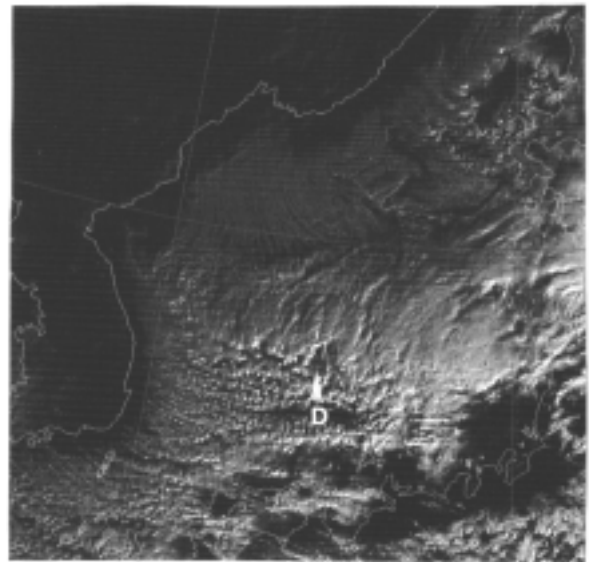


Figure 6-2-4 b. VIS image at maturity at 00UTC, January 24, 1998.
Symbols: Refer to the text.

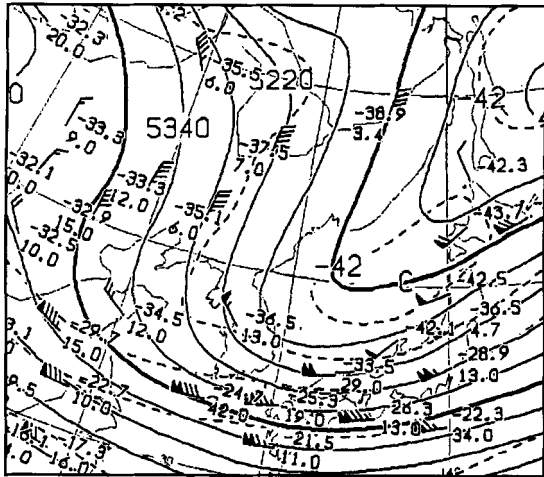


Figure 6-2-4 c. 500 hPa weather chart at 00UTC, January 24, 1998

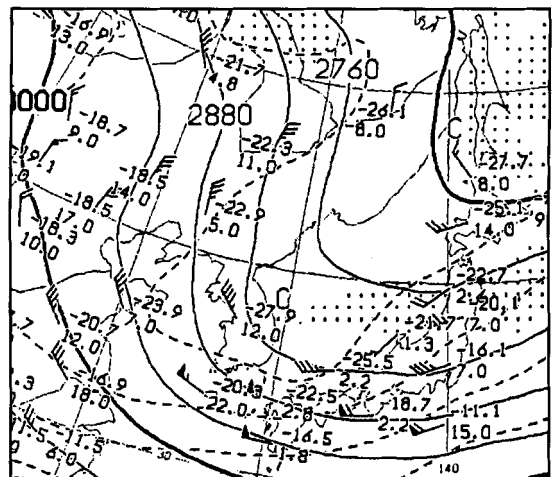


Figure 6-2-4 d. 700 hPa weather chart at 00UTC, January 24, 1998

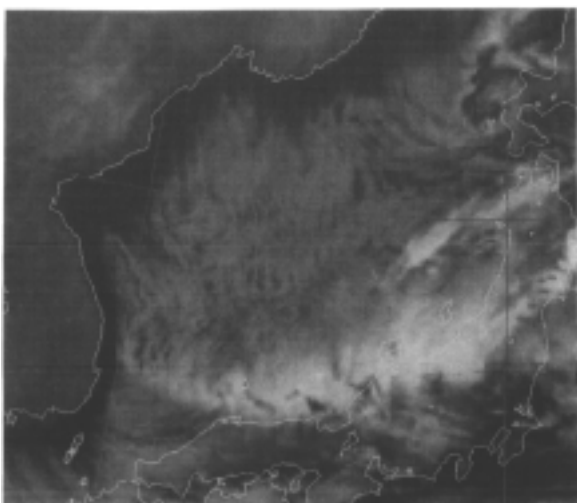


Figure 6-2-5 a. IR image at maturity at 06UTC, January 24, 1998
Symbols: Refer to the text.

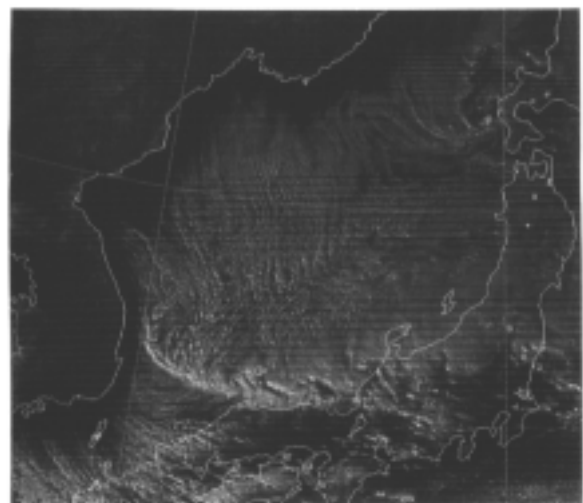


Figure 6-2-5 b. VIS image at maturity at 06UTC, January 24, 1998
Symbols: Refer to the text.

(3) Decaying stage

At 12UTC, 24th, the convective cloud belt move south further and landed San'in District with its Cg and Cb accompanying. The low-level vortex D landed Hokuriku District and dissipated. In the districts where landed, an intense snowfall of 5 to 9 cm per hour was observed. After having landed, the convective cloud belt could not get across the spinal ridges of the Japanese Islands and decayed while it lowered its top height gradually. On the north of this convective cloud belt, a cloud street having a meridional direction prevails. At this time, a trough at 500 hPa lay in Tohoku District, and a thermal trough at -24°C at 700 hPa in Hokuriku District (Figure 6-2-6).

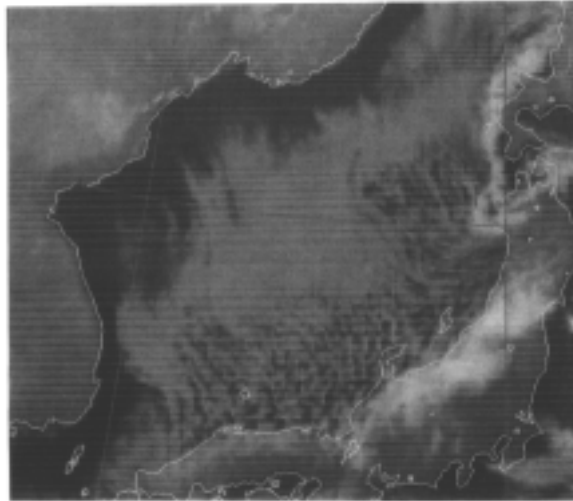


Figure 6-2-6 a. IR image at decaying stage at 12UTC, January 24, 1998
Symbols: Refer to the text.

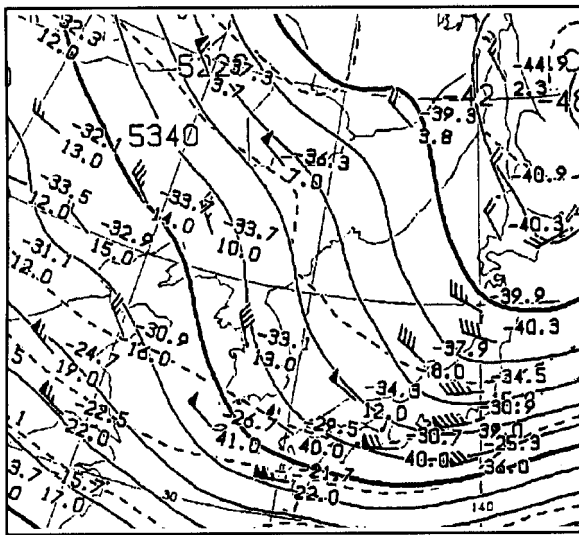


Figure 6-2-6 b. 500-hPa weather chart at 12UTC, January 24, 1998

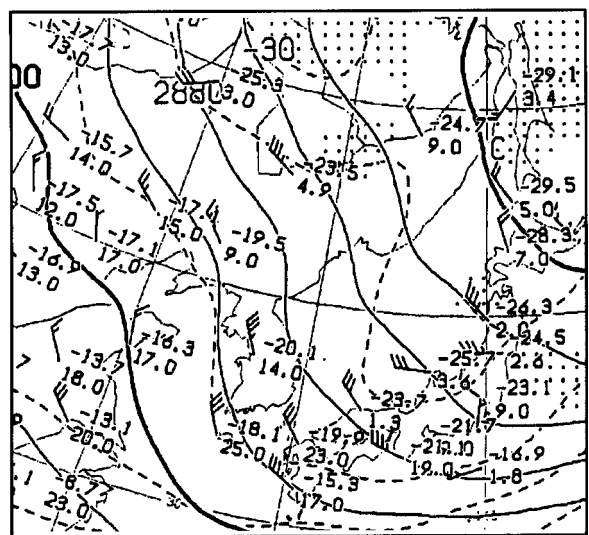


Figure 6-2-6 c. 700-hPa weather chart at 12UTC, January 24, 1998

(4) Summary

The changes and movements of the convective cloud belt in this example are summarized as follows:

- ① The convective cloud belt originated in the western Sea of Japan, and began to elongate to the southeast while it was increasing the cloud top height.
- ② After that, a low-level vortex appeared on the convective cloud belt, and a difference was seen in tangential direction of the convective cloud belt between in front of and behind this low-level vortex.
- ③ The convective cloud belt runs nearly west to east in front of the low-level vortex and lands the coast of Hokuriku to Tohoku District. After landing, it cannot get across the spinal ridges and dissipates. Snowfall intensifies around the point of landing.
- ④ The convective cloud belt begins to move south behind the low-level vortex, and its direction turns gradually to an east to west direction. The portion behind the low-level vortex moves south further and dissipates after it lands San'in to Hokuriku District. Snowfall intensifies around the point of landing.

6.2.2 Hokkaido west coast small low

The sea area sandwiched between the Maritime Territory and Sakhalin and Hokkaido (and the sea ice field of the Sea of Okhotsk) becomes relatively warm in the winter and forms a pressure trough. In the area from the Tatar Strait to the northern Sea of Japan, the northwest monsoon blowing out of the continent collides with the northeast wind blowing out of cold Sakhalin, Hokkaido (and the sea ice field of the Sea of Okhotsk) to form a convergence line running north to south. A field of ascending current forms above this convergence line and a cloud band appears (Figure 6-2-7). When an upper trough approaches this cloud band, the ascending current intensifies and a low-level vortex containing active convective clouds appears. Then, a small low, or a pocket-like area of low pressure comes to be analyzed. This mesoscale low-level vortex appears on the west coast of Hokkaido, so it is called the Hokkaido west coast small low. Of these, the one appearing in the Ishikari Bay is called the Ishikari Bay small low. The mesoscale low-level vortex moves south with the northern current of northwest and northeast winds and lands western Hokkaido or northern Tohoku District, causing heavy snow there very often.

For the Hokkaido west coast small low, there is a report (1989) by the Sapporo District Meteorological Observatory, and it has been investigated from various aspects. Of these, the points on satellite imagery investigation are broadly divided into the cloud band type and vortex cloud type (Okabayashi, 1972), and both types are further divided into a total of 7 groups. Flow charts of origination, snow storm prediction work sheets and the like have been prepared by the types. This section takes up an example of the Hokkaido west coast small low and lists the points on satellite imagery.

(1)

A mesoscale low-level vortex appeared at southern Sakhalin at 18UTC, December 20, 1997. Under the influence of an upper vortex, it developed over the sea waters southeast of Wakkanai to become distinct. After that, this vortex moves south together with spirally arranged

cumulonimbus clouds encircling around the periphery of the vortex. It landed Ishikari District and brought about heavy snow at and around Sapporo.

The path of the low-level vortex analyzed from satellite imagery and the path of the upper vortex derived from the water vapor imagery are shown in Figure 6-2-8.

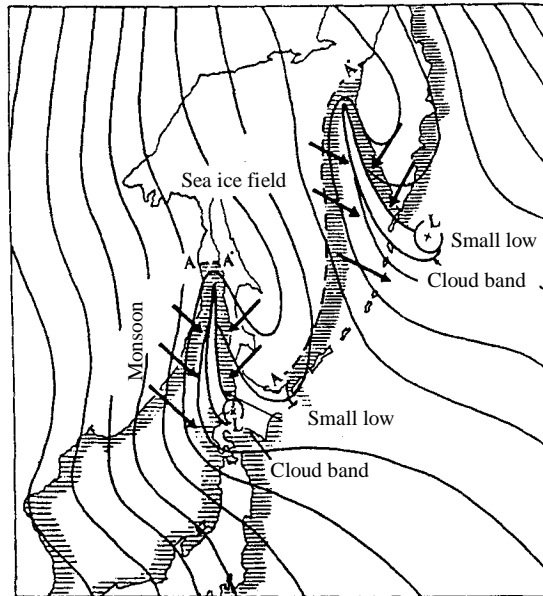


Figure 6-2-7. Schematic model for appearance of cloud band and small low (Okabayashi, 1972)

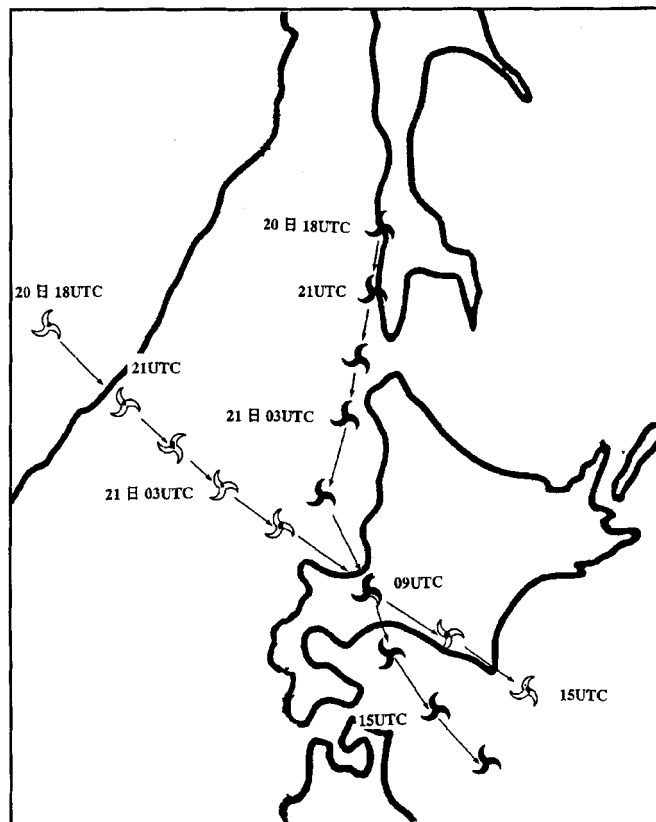


Figure 6-2-8. Paths of lower level and upper vortices analyzed from satellite image
 S: Low-level vortex (positions at 3-hour intervals) L: Upper vortex (positions at 3-hour intervals)

① Before appearance of low-level vortex

Hokkaido District is covered by a hibernal “west-high, east-low” pressure pattern (Figure 6-2-9). In the infrared imagery, the northern Sea of Japan is behind a low and is covered by a convective cloud area A whose convective activity is feeble (Figure 6-2-10).

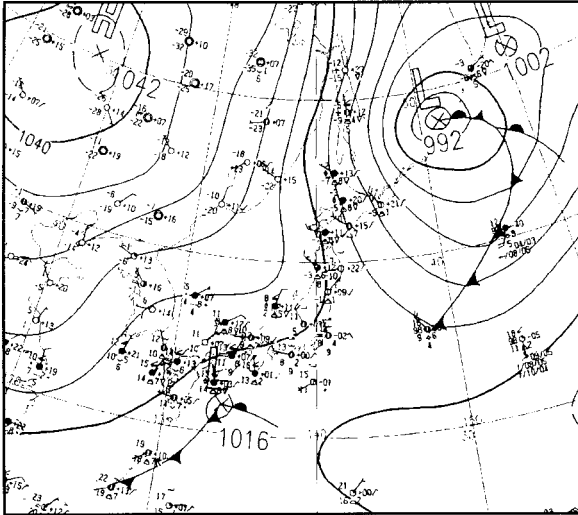


Figure 6-2-9.
Surface weather chart at 12UTC,
December 20, 1997

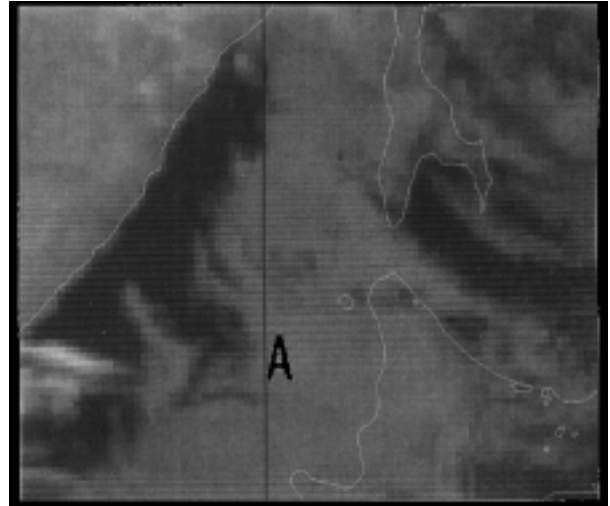


Figure 6-2-10.
IR image taken before appearance of low-level
vortex at 12UTC, December 20, 1997

② Low-level vortex at formative stage

In the water vapor imagery (Figure 6-2-11), the upper vortex B, which had lain around Siberia, moved east-southeast and reached the Maritime Territory. This upper vortex is accompanied by cold air at -42°C at 500 hPa and is associated with a positive vorticity of 227 (Figure 6-2-12). A low-level vortex C (vortex center marked by X) appeared in southern Sakhalin when this upper vortex came close. Cold air intensified from the northern Sea of Japan to the Tatar Strait, and the convective cloud area A enlarged with the result that the coastal gap from the continent was narrowed (Figure 6-2-13).

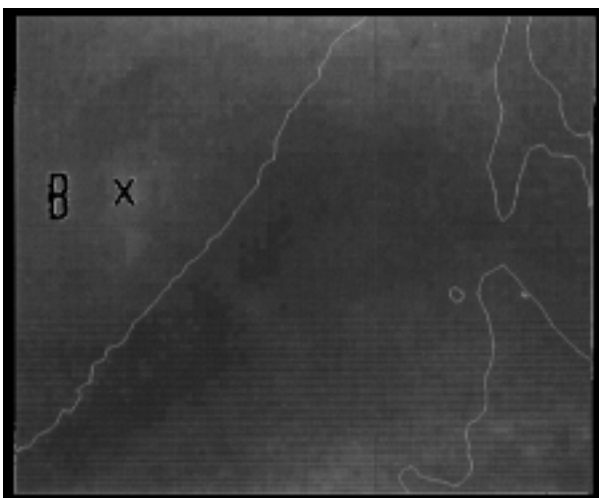


Figure 6-2-11.
WV image of low-level vortex at formative stage at
18UTC, December 20, 1997

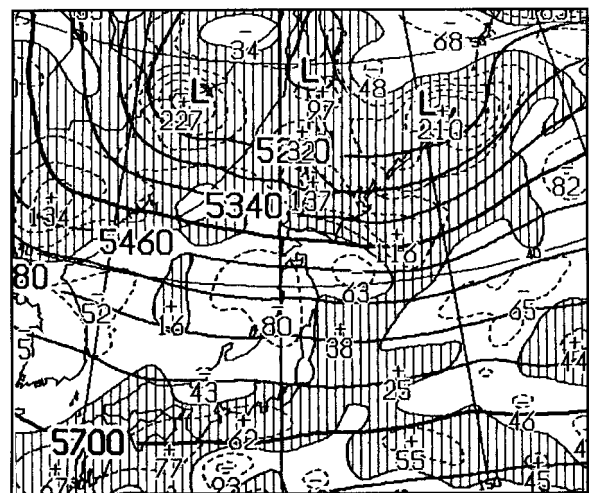


Figure 6-2-12.
500-hPa geopotential height and vorticity analysis
chart at 12UTC, December 20, 1997

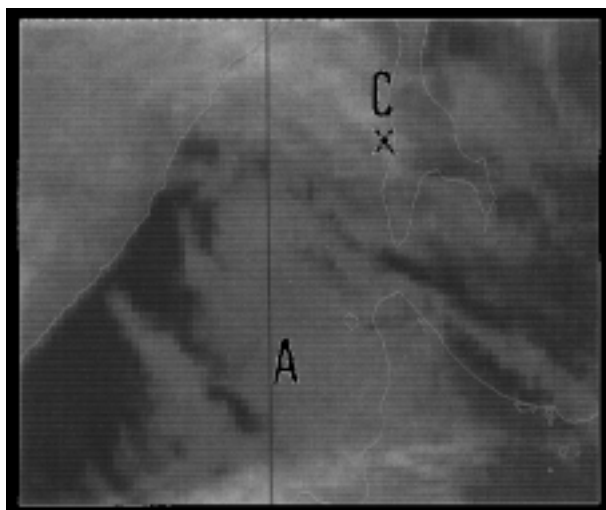


Figure 6-2-13. IR image of low-level vortex at formative stage at 18UTC, December 20, 1997

③ Low-level vortex at developing stage

As the upper vortex came close, the convective activity of the cloud line encircling the low-level vortex C was activated and came to contain Cb. The convective cloud A in the northern Sea of Japan assumed a striated structure, indicating an intensified wind speed. The coastal gap narrowed further (Figure 6-2-14).

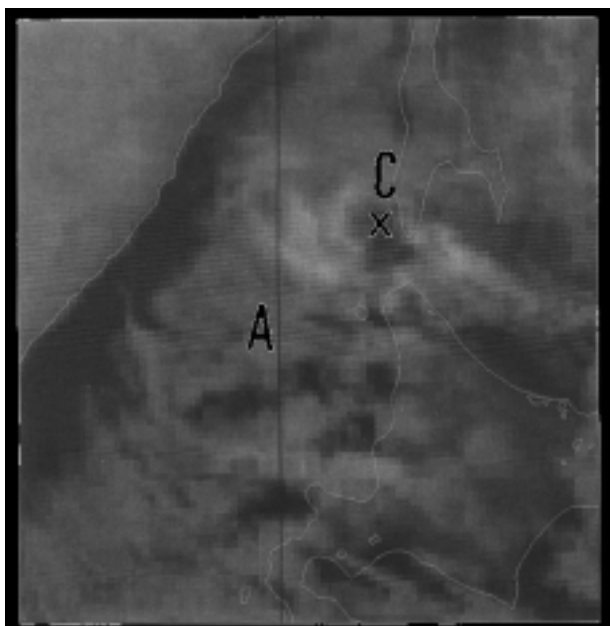


Figure 6-2-14. IR image of low-level vortex at developing stage at 00UTC, December 21, 1997

④ Low-level vortex at maturity

The Cb clouds encircling the low-level vortex C assumed spiral form. According to a temperature distribution chart prepared by infrared imagery, the low-level vortex had a fair area about 80 km in diameter. The fair area is encircled by Cb clouds around, which has a cloud top temperature of about -40°C (cloud top height about 4,800 m), and convective activity has been activated there. In the visible imagery as well, the center of the low-level vortex forms a fair area at this time. Figure 6-2-17 shows a wind direction and rainfall distribution map prepared by AMEDAS, showing

cyclonic rotation of the low-level winds around the low-level vortex C over the sea waters southwest of Wakkanai.

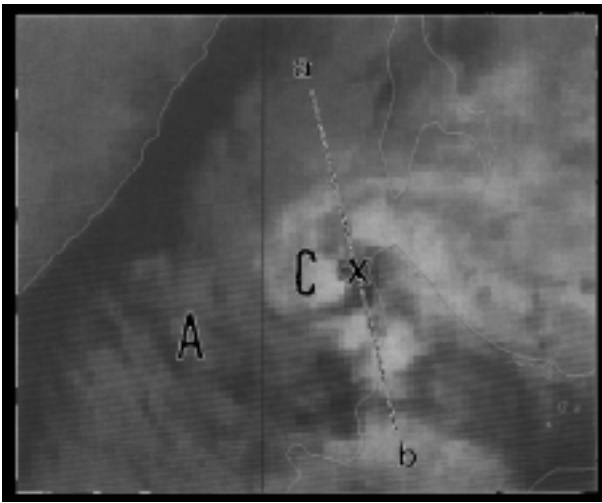


Figure 6-2-15 a. IR image of low-level vortex at maturity at 03UTC, December 21, 1997

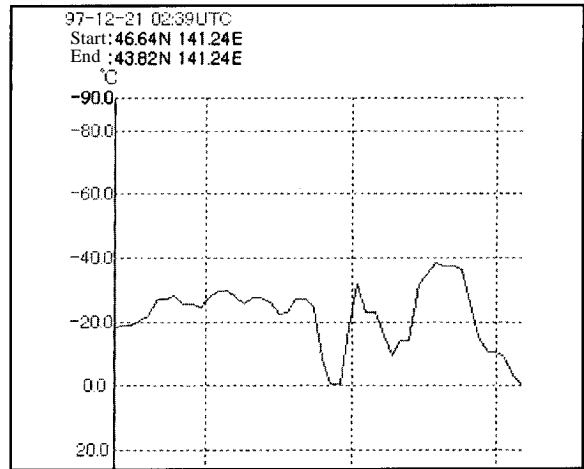


Figure 6-2-15b. Infrared temperature distribution along a-b at 03UTC, December 21, 1997

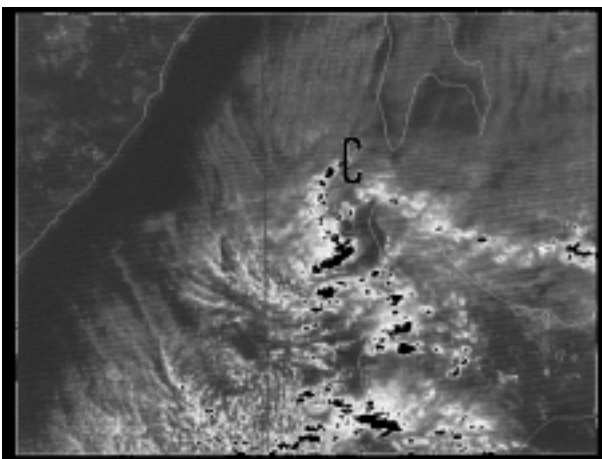


Figure 6-2-16. VIS image of low-level vortex at maturity at 03UTC, December 21, 1997

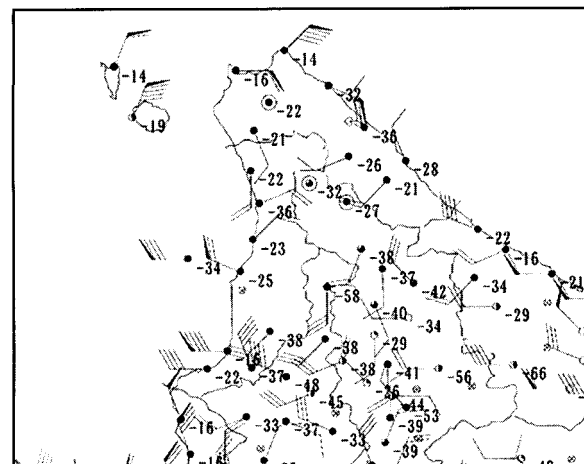


Figure 6-2-17. Wind direction and speed and rainfall distribution map by AMEDAS at 03UTC, December 21, 1997

⑤ Low-level vortex at decaying stage

At 09UTC, 21st, the low-level vortex C lay directly under the upper vortex and had somewhat lowered its cloud top height. It landed around Sapporo. The Cb clouds encircling the low-level vortex became a bow-shaped convective cloud line D under the influence of the topography in the Ishikari Bay, and part of them landed Ishikari District. At Sapporo, a snowfall of 10 cm was observed from 12UTC, 21st to 00UTC, 22nd. In the radar composite chart (Figure 6-2-18), the echo clusters are bow-shaped and there are intense echoes around the Shakotan Peninsula. The coastal gap of the convective cloud A from the continent has widened, and the cold air is getting weak (Figure 6-2-19).

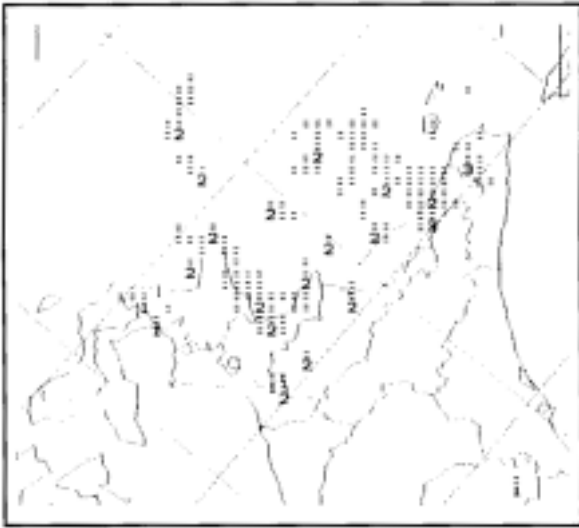


Figure 6-2-18. Radar composite chart at 18UTC, December 20, 1997

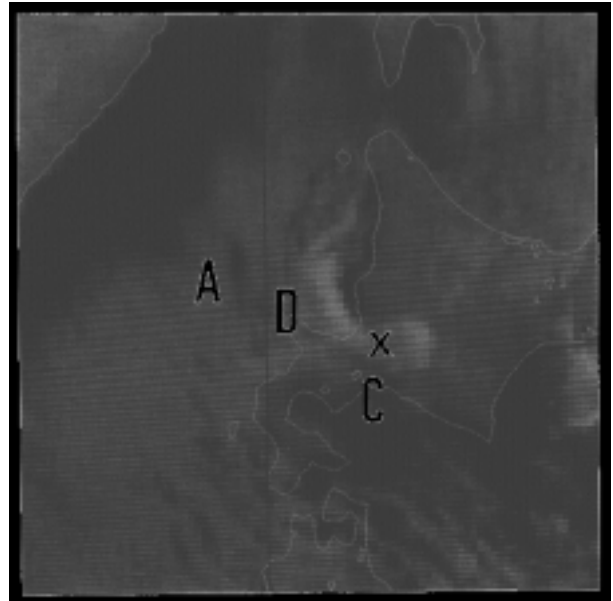


Figure 6-2-19. IR image of low-level vortex at decaying stage at 09UTC, December 21, 1997

⑥ Low-level vortex at dissipating stage

The upper trough passed into the sea to the east ahead of the low-level vortex, and the low-level vortex left over became indistinct. The cloud top height around the vortex further lowered (Figure 6-2-20).

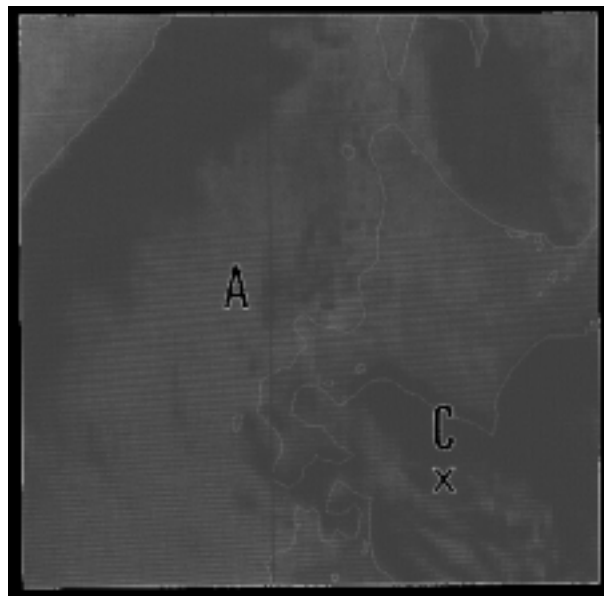


Figure 6-2-20. Infrared imagery of low-level vortex at dissipating stage at 15UTC, December 21, 1997

(2) Points on satellite imagery

- ① In Sakhalin, Hokkaido (and the sea ice field), the area of high pressure intensifies by radiation cooling in the night. The northeast wind flowing out there collides with the northwest monsoon and forms a convergence line from southern Sakhalin to the Soya Strait.

- ② A low-level vortex appears when an upper trough comes close to the sea waters west of southern Sakhalin and Hokkaido. The low-level vortex becomes a vortex of active convective clouds, and a small low or a pocket-like area of low pressure comes to be analyzed.
- ③ The northeast and northwest winds move south while they merge. The cloud band (low-level vortex) exhibits a cyclonic curvature (to the left looking in the moving direction) while it moves south, and causes heavy snowfall around the point of its landing (hatched area in Figure 6-2-21).
- ④ When the low-level vortex is passed by an upper trough, it weakens in convective activity and loses its shape.

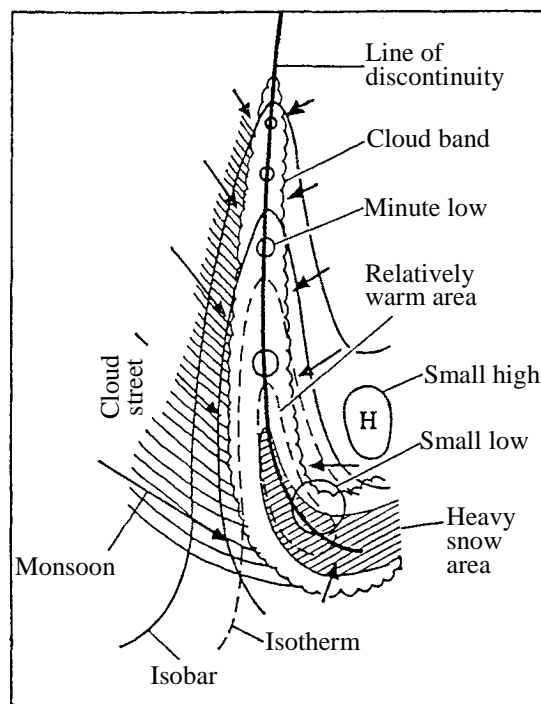


Figure 6-2-21. Schematic model for convergence line formation and snowfall mechanism (Okabayashi, 1972)

6.2.3 Features of hibernal pressure pattern

In the winter, a cloud street appears over the Sea of Japan associated with the hibernal pressure pattern. The direction of the cloud street is related with snowfall on the Sea of Japan coast. This section describes the relation between the direction of cloud street and snowfall distribution as well as the isobars on the surface weather chart.

- (1) When the isobars run north to south, on January 22, 1997 (Figure 6-2-22)

In the visible and infrared imageries at 9, 22nd, a cloud street spreads over the Sea of Japan and part of it gets through Sekigahara and the Kii and Bungo Straits into the Pacific Ocean where deep cloud streets are seen. By the influence of this cloud street getting through into the Pacific, there was a record snowfall at Yokkaichi City, Mie Prefecture. A cloud line of high brightness is seen running east to west around Hachijo Island. A snowfall due to this cloud line was observed there for the first time in 16 years.

There were lows around Hokuriku and off Sanriku at 9, 21st. and they merge over the ocean waters east of Japan at 9, 22nd to form an intense hibernal pressure pattern around Japan. The isobars around Japan turned to run north to south.

The snowfall due to this hibernal pressure pattern was centered on Hokuriku to San'in District.

Major observed records of snowfall for 24 hours to 9, 22nd are as follows:

- Kotani-mura, Nagano Prefecture: 67 cm
- Tsunan-machi, Niigata Prefecture: 62 cm
- Yokkaichi City, Mie Prefecture: 21 cm
- Sasayama-machi, Hyogo Prefecture: 35 cm
- Takano-machi, Hiroshima Prefecture: 56 cm

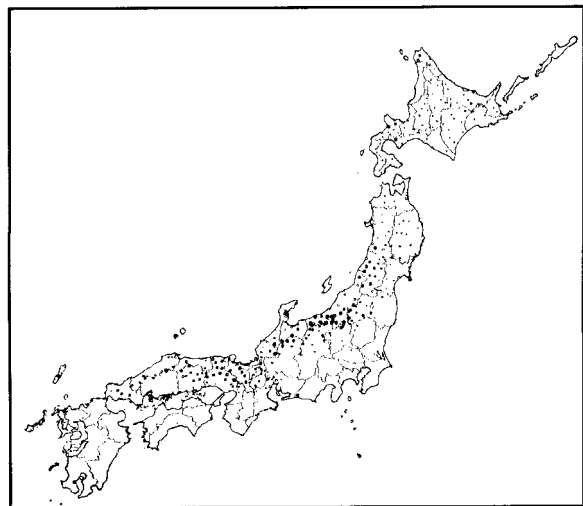
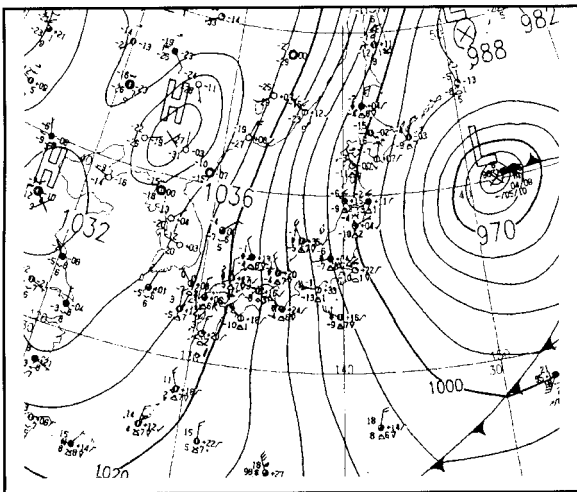
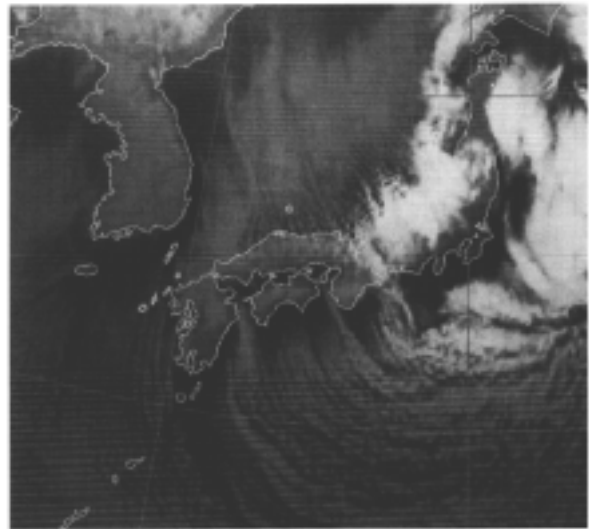
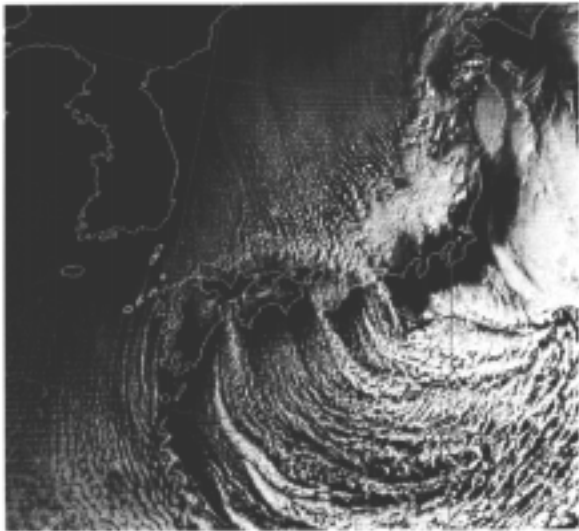


Figure 6-2-22. Cloud street of meridional direction at 9, January 22, 1997

Top left: VIS image Top right: IR image

Bottom left: Surface weather chart Bottom right: 24-hour snowfall in whole Japan

(2) Isobars running west to east in January 20, 1998 (Figure 6-2-23)

In the visible and infrared imageries at 9, 20th, there was a cloud street with an east-west direction. The cloud street landed from the Noto Peninsula to the Sea of Japan coast of Tohoku district, and it contains Cu and Cg there. Under this cloud area, there was much snowfall.

There was a low over the ocean waters east of Kanto at 9, 19th, and it moved far off the sea east of Japan at 9, 20th. Part of a high over the continent extended from southern China, and a weak hibernal pressure pattern prevailed around Japan with a pressure trough left over in the western Sea of Japan. The isobars in the northern Sea of Japan ran from northwest to southeast. In the central and western Sea of Japan, the pressure gradient eased and the isobars ran in a nearly east-west direction.

Major observed records of snowfall for 24 hours to 5, 20th are as follows:

- Hijiori, Okura-mura, Yamagata Prefecture: 73 cm
- Kuzuryu, Izumi-mura, Fukui Prefecture: 65 cm
- Itani, Hosoiri-mura, Toyama Prefecture: 49 cm
- Nagataki, Shiratori-machi, Gifu Prefecture: 44 cm
- Tsugawa-machi, Niigata Prefecture: 42 cm

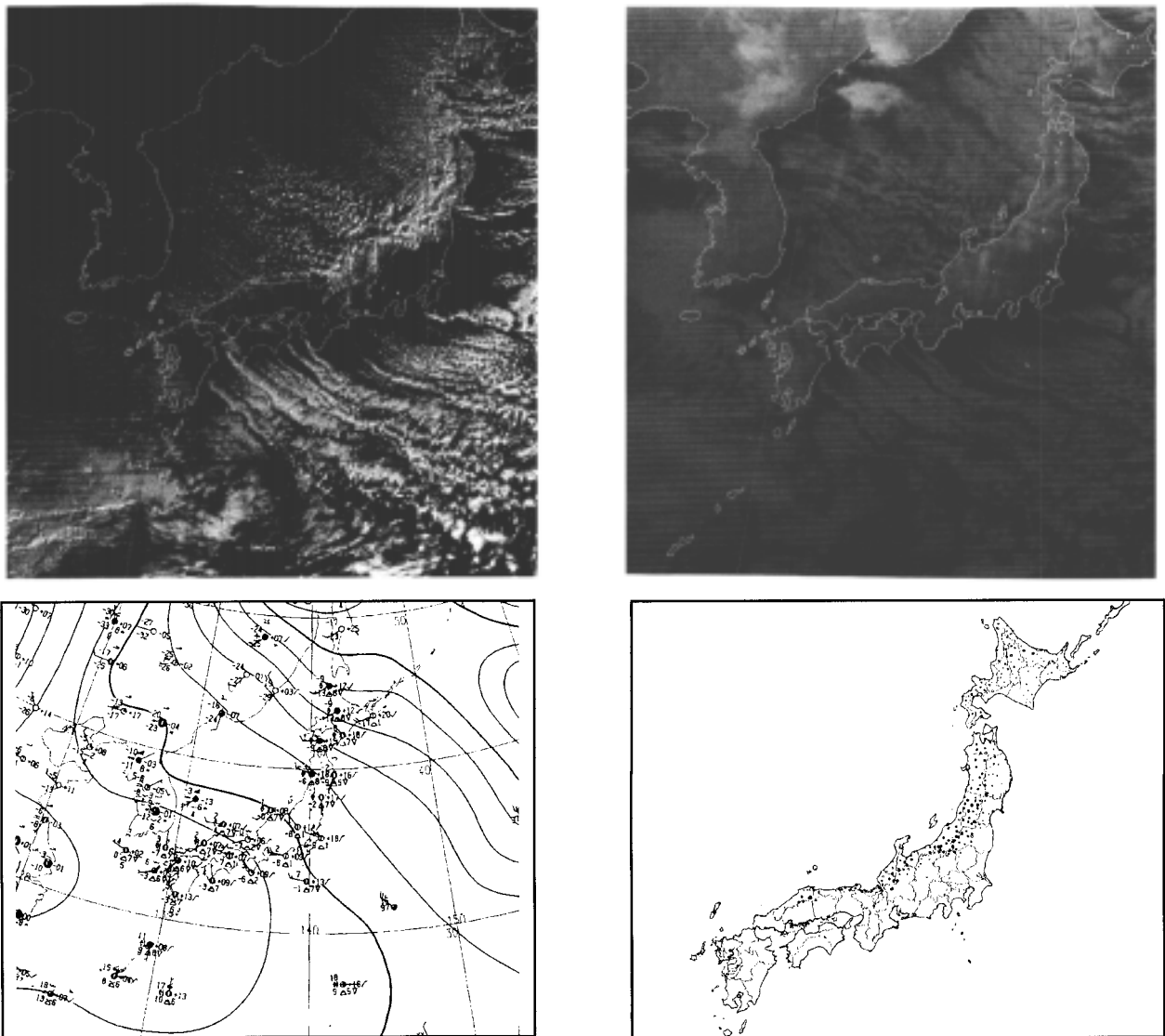


Figure 6-2-23. Cloud street running west to east at 9, January 20, 1998

Top left: VIS image Top right: IR image

Bottom left: Surface weather chart Bottom right: 24-hour snowfall in whole Japan

(3) Isobars running from northwest to southeast in January 9, 1999 (Figure 6-2-24)

In the visible and infrared imageries at 9, 9th, a convective cloud belt is seen in part of the western Sea of Japan. Except for this, however, the entire Sea of Japan is filled with cloud street running

from northwest to southeast. Cg is also seen all over the Sea of Japan. The direction of the cloud street somewhat differs from that of the isobars. The cloud street blows through also to the Pacific coast of northern, eastern and western Japan.

At 9, 9th, there was a slow-moving low over the Sea of Okhotsk, and there was a strong high over the continent. An intense hibernal pressure pattern had continued around Japan since the early dawn of the 7th. The isobars around Japan ran nearly from northwest to southeast from the Sea of Japan to the ocean waters east of Japan.

The snowfall due to this hibernal pressure pattern was centered on the Sea of Japan coast widely from Hokkaido to San'in District.

Major observed records of snowfall for 24 hours to 16, 9th are as follows:

Suijo(u), Ibuki-machi, Shiga Prefecture: 71 cm

Sekigahara, Gifu Prefecture: 63 cm

Fujiwara, Minakami-machi, Gunma Prefecture: 69 cm

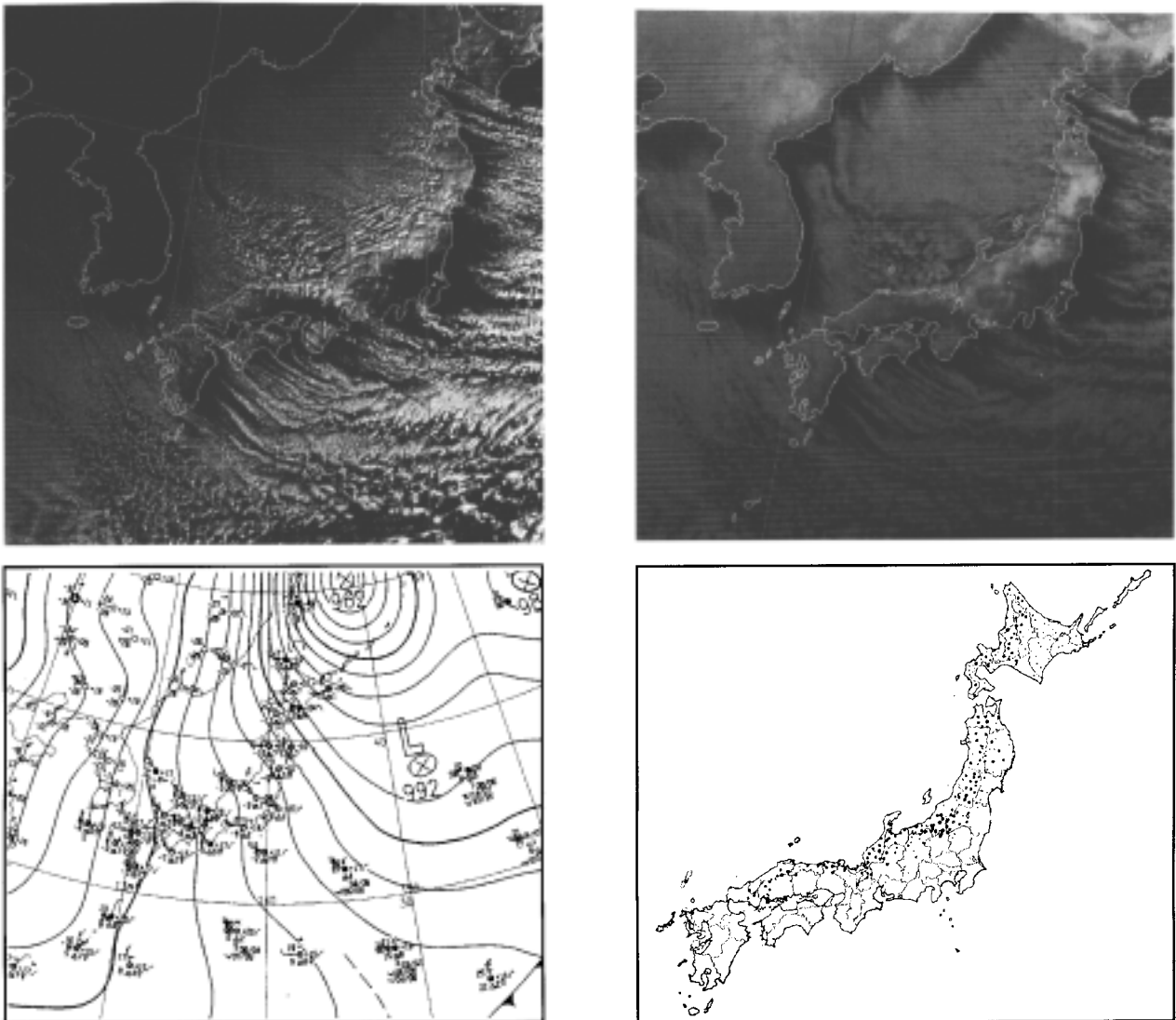


Figure 6-2-24. Cloud street from northwest to southeast at 9, January 9, 1999
Top left: VIS image Top right: IR image
Bottom left: Surface weather chart Bottom right: 24-hour snowfall in whole Japan.

6.3 Strong wind

To draw information on winds from satellite imagery, it is general practice to track the cell of a cloud using multiple images and calculate its movements. Besides this, characteristic cloud patterns appear associated with a strong wind. For example, there are reports saying, “A convective cloud appears associated with a cold air outbreak. If it becomes a cloud line in striated form, then the surface wind speed is 20 kt or higher” (Meteorological Satellite Department, 1976), and “If it comes that lee wave cloud appears on the lee of a mountain ridge, there is a wind speed of 20 kt or over near the ridge. The intervals of cloud lines of lee wave cloud are proportional to wind speed, that is, wider cloud line intervals result for a higher wind speed” (Obana, 1983).

This section takes up the strong wind at the passage of a cold front in the hibernal pressure pattern in the cold season, and gives an example of drawing information about winds at low levels.

6.3.1 Strong wind at passage of cold front

On February 27, 1999, there was a low over the sea west of Hokkaido and it moved east-northeast over Hokkaido while it was developing. Therefore, the pressure pattern changed into the hibernal pattern and northwest strong winds began to blow in Kanto District from the evening of the 27th.

(1) When the cold front lay over the Sea of Japan

In the surface weather chart at 00UTC, 27th (Figure 6-3-1), there is a surface low around Wakkanai and a cold front extends to northern Kyushu. There is another low over the sea east of Kanto, and a cold front extends from there and reaches southern China through the Nansei-shoto Islands.

Of these, pay attention to the cold front over the Sea of Japan coast. Figure 6-3-2 shows the visible image at that time. A Cg-Cu line (A-B) extending from off Akita to off San'in can be analyzed behind the cold front extending over the Sea of Japan coast. The Cg-Cu line is moving east-southeast at 20 m/s near the portion marked by an arrow. Over the central Sea of Japan behind the cold front, a striated convective cloud (C) has appeared and this convective cloud cell is moving south-southeast at 15 m/s.

From these, a strong west-northwest wind is estimated behind the cold front. According to the AMeDAS time-series chart (Figure 6-3-3) at Aikawa (Niigata), the time of passage of the cold front at Aikawa was around 01UTC (10JST), 27th when the air temperature fell. Around 03UTC (12JST), the wind speed intensified from 9 to 18 m/s. This wind speed almost agrees with the movement of cloud street cell. It also almost agrees with the moving speed of the Cg-Cu line (A-B) near the portion marked by an arrow.

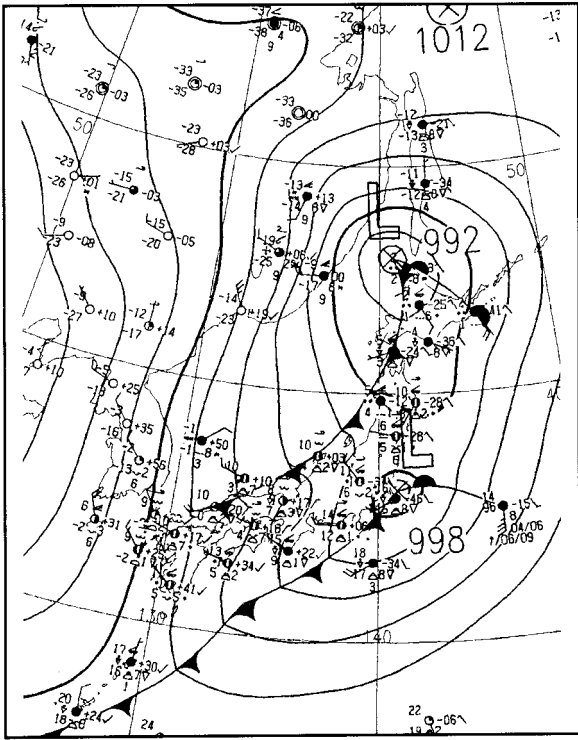


Figure 6-3-1.
Surface weather chart at 00UTC, February 27, 1999

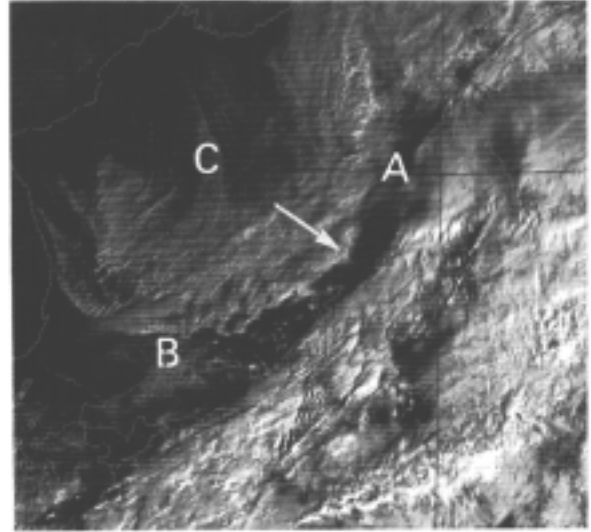


Figure 6-3-2.
Visible image at 00UTC, February 27, 1999
Symbols: Refer to the text.

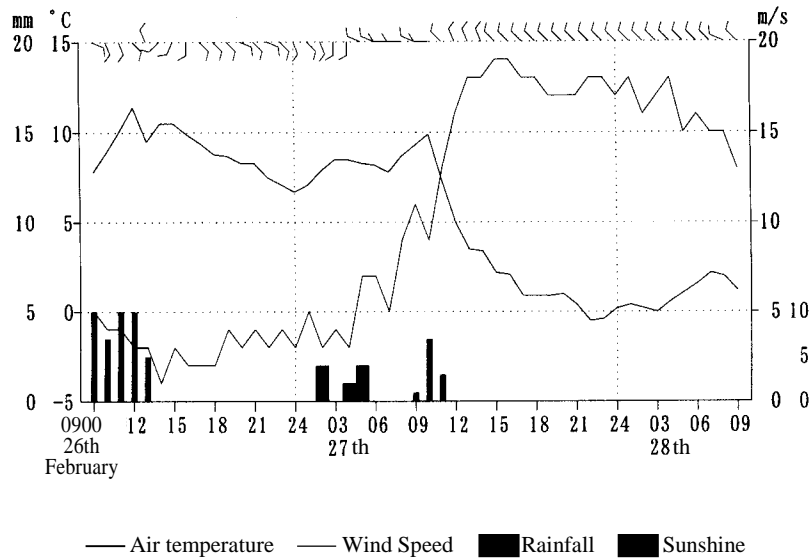


Figure 6-3-3.
AMeDAS time-series chart at Aikawa (Niigata) from 09JST, February 26 to 09JST, February 28, 1999

(2) When the cold front lay inland

The Cg-Cu line (A-B) became indistinct when it passed over the spinal mountains and it became indiscernible on the satellite image. We estimate here the time of passage of the cold front over Kanto District from an AMeDAS time-series chart. The AMeDAS time-series chart at Tokyo is shown in Figure 6-3-4. At 0630UTC (1530 JST), 27th, a rapid shift in wind direction (from east-southeast to west-northwest) was seen. The wind speed intensified from 3 to 11 m/s at

0710UTC(1610 JST), and the air temperature began to fall with a peak at that time. From these, the passage of the cold front at Tokyo is estimated at around 0700UTC(1600 JST), 27th.

Let us see the features at the passage of a cold front on the visible image (Figure 6-3-5) at 07UTC around which the cold front passed over. The Cg-Cu line (A-B), which had lain over the Sea of Japan coast, landed and became indistinct. Cu (D) appeared over the Chubu and Tanzawa Mountains, which had been fair until 06UTC. Lee wave cloud (F) appeared over the Pacific coast of Tohoku District and the east side of Kii Peninsula. Beside these, a cloud street (E) running from east to west is also seen off Sanriku. From these, a strong west wind can be estimated around there.

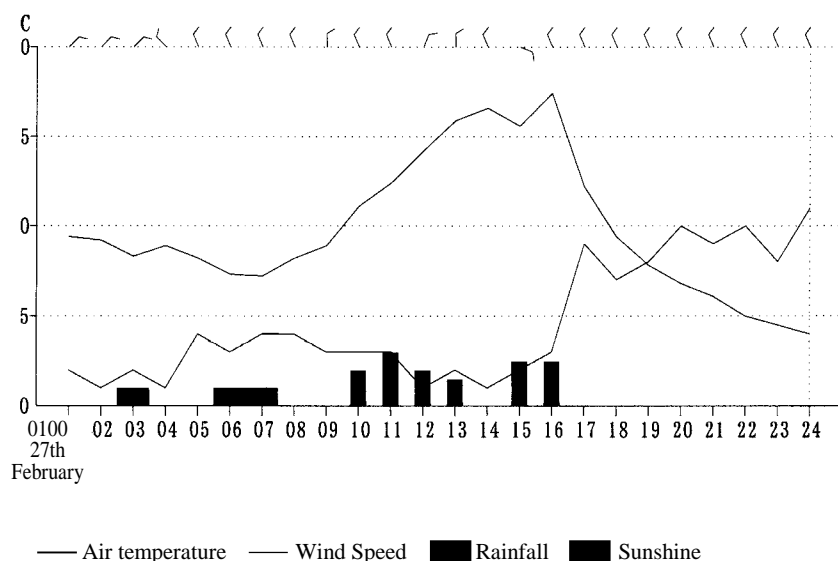


Figure 6-3-4. AMeDAS time-series chart at Tokyo from 01JST to 24JST, February 27, 1999

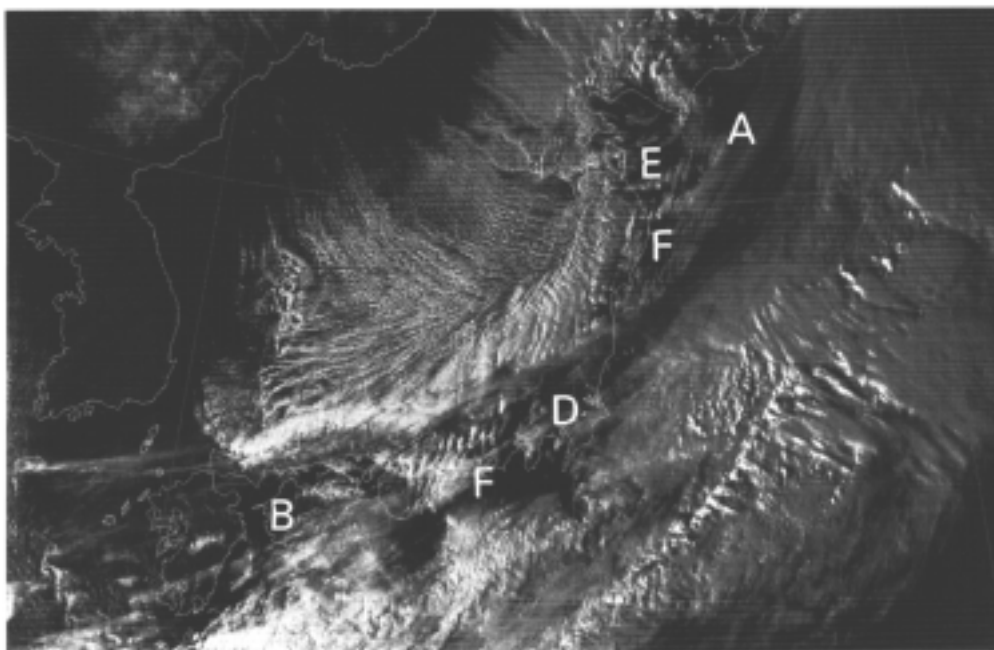


Figure 6-3-5. Visible image at 07UTC, February 27, 1999
 Symbols: Refer to the text.

Wind speed can be estimated from these features on the image. Because the intervals of cloud lines of lee wave cloud are proportional to wind speed, the latter can be estimated from the former (see Section 3.7). Let us apply G.A. Corby's relationship (1957)

$$\text{Wind speed } U \text{ (m/s)} = 1.7\lambda \text{ (km)} + 4.8$$

to this example. Then, the wind speed is 18.4 m/s if the wavelength λ of the lee wave is 8 km.

The position of the cold front analyzed from the image at 07UTC, 27th is shown in Figure 6-3-6 together with the wind vectors at low levels derived from the convective cloud cell movements as well as the appearance of cloud street and lee wave cloud.

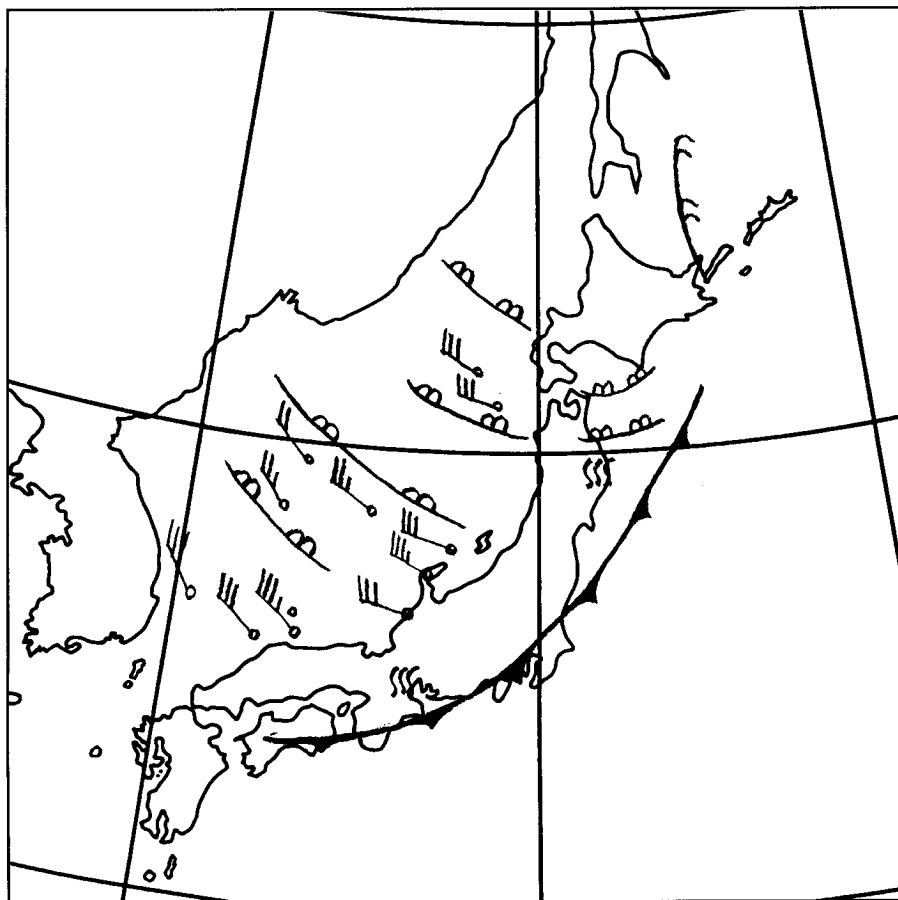


Figure 6-3-6. 07UTC, February 27, 1999
(Position of the cold front analyzed from the image and low-level wind vectors derived from the movements of convective cloud cells as well as striated cloud and undulatus)

▲ : Cold front ≡≡≡ : Undulatus ~~~ : Striated cloud ↙ : Low-level wind vector

(3) When the cold front passed into the Pacific Ocean

According to the visible image (Figure 6-3-7) at 01UTC, 28th, after the front had passed the Japanese Islands, fair weather peculiar to the hibernal pressure pattern prevails over the inland of Kanto District, off Sanriku and off southeast of the Kii Peninsula under the influence of the spinal mountains. On the other hand, striated convective cloud lines (F) blowing through from the Sea of

Japan to the Pacific lie over Hokkaido and Tohoku and Kinki Districts under the influence of cold air and strong winds. At this time, winds at low levels derived from the convective cloud cell movements on the Pacific side were west-northwest at 15 m/s off Sanriku and west-northwest at 13 to 15 m/s over the sea east of Kanto.

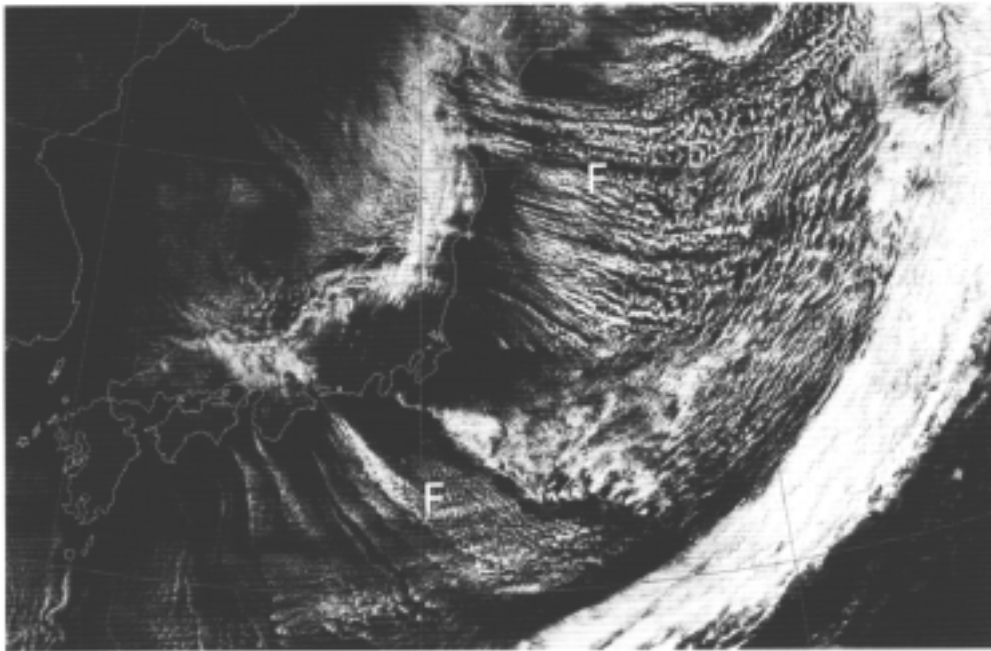


Figure 6-3-7. Visible image at 01UTC, February 28, 1997
Symbols: Refer to the text.

6.3.2 Points on the image at strong wind and their use

- (1) Cu appears associated with a cold air outbreak begins to assume striated form when the surface wind speed exceeds 20 kt. The surface wind speed on the land or sea can be estimated by finding the movements of individual cells of this cloud street and calculating the wind speed at low levels. Because cloud street is formed as cloud lines parallel to the surface wind direction on the land or sea, the surface wind direction can be estimated from the direction of cloud street (Meteorological Satellite Department, 1976).
- (2) Lee wave cloud appearing on the lee of a mountain range indicates a wind speed of 20 kt or over near the mountain ridge. Because the intervals of cloud lines of lee wave cloud are proportional to wind speed, that is, the intervals of cloud lines of lee wave cloud are wider at higher wind speeds, wind speed can be estimated from the intervals (Obana, 1983).

6.4 Fog and low cloud

6.4.1 Fog

(1) General features of fog

Because the satellite observes the cloud tops, it is impossible to distinguish fogs with its bottom touching the ground from low-level stratus which doesn't touch the ground on the satellite imagery. Therefore, the two are treated equally as fog in nephanalysis. Their features are described below.

In the infrared imagery, fog appears dark gray or a still darker tone. Because its top is low and there is little temperature difference with the surrounding ground (or sea) surface, it is difficult to identify a fog area on the infrared image. Fog existing when an intense ground inversion is present is called the Black Fog because its top temperature is higher than the ground surface temperature around it and it appears darker than the surrounding fog-free ground surface on the infrared image (Bader et al., 1995)

Fog is seen as a gray or white area in the visible image. The top surface of a fog area is smooth and uniform. The top height is almost constant, so the boundary of a inland fog area shows a shape along a contour in many cases. Identification of a fog area is easy on the visible image unless it is covered by a thick high or middle cloud. Identification of fog is generally possible even when it is covered by a see-through thin high clouds. However, if a granular high clouds cover, it casts its shadow on the surface of the fog area, so the fog may be mistaken for a rugged convective cloud. In general, fog is slow in movement and changes its shape slowly. Therefore, it is also effective for identification of fog to ascertain the movements and changes in shape on the animation images.

Fog thickness is generally several hundred meters or less. Therefore, if there is an obstacle such as a mountain and hill that is higher than the fog thickness, a fog-free gap may appear on the lee of the obstacle. From this, an approximate wind direction there can be estimated.

(2) Sea fog

Figure 6-4-1 shows an example of occurrence of fog widely around Japan. On the visible image, a fog area is a white or bright white region with a smooth surface, and such a region is recognized from the Pacific coast of Hokkaido and Tohoku District to the sea area to the east (A), in the northern and central Sea of Japan (B) and around the east coast of the Korean Peninsula (C). A dark gray small fog area is recognized on a coastal area of the western Korean Peninsula (D) and in the Yellow Sea (E). The fog area (A) intrudes into the inland of the Tokachi Plain, and a distinct border is seen at the Hidaka Mountains in Hokkaido. On the infrared image, these fog areas cannot be clearly identified on the sea. In contrast, on the land of Hokkaido, the ground surface temperature rises by sunshine in the cloud free area and the temperature difference between ground surface and fog top becomes large. Therefore, the border of the fog area is distinct. The cloud area (F) on the Pacific coast of Tohoku District appears to be a fog. On the visible image, however, it can be identified as a cloud (Sc or Cu) different from a fog since it is brighter and more rugged than the fog area in Hokkaido.

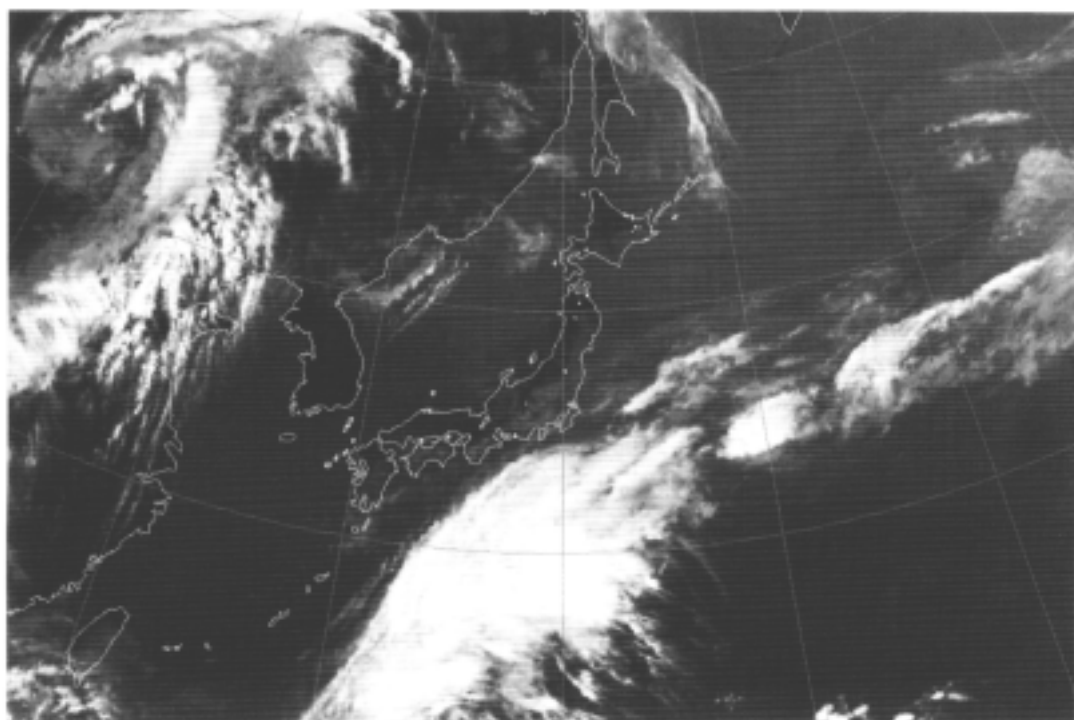
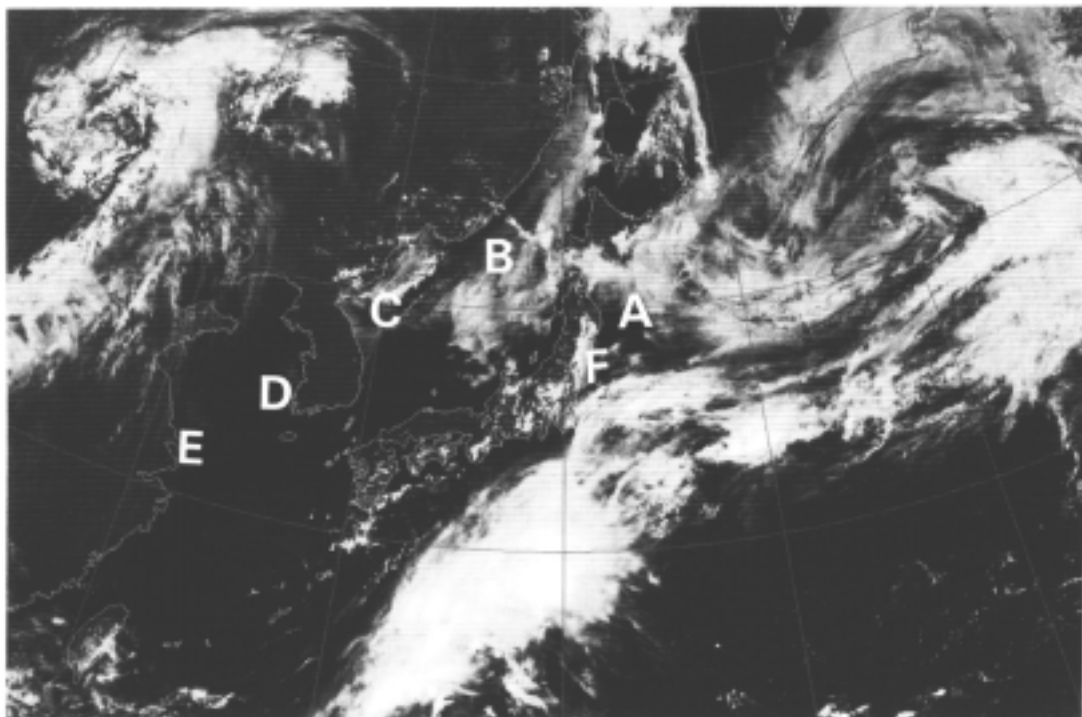


Figure 6-4-1. Sea fog at 03UTC, June 17, 1997.
 Top: Visible image. Bottom: Infrared image. Symbols: Refer to the text.

Figure 6-4-2 shows an example of a fog blocked by an obstacle. There is a fog about 100 km wide along the Kuril Islands and on the Sea of Okhotsk side. This fog flows into the Pacific through between islands, indicating that the west or northwest wind flowing to the cyclone east of Kamchatka Peninsula prevails at the northern Kuril Islands. Since the border of the fog area that flowed out is not disturbed, the wind speed is estimated to be weak. On the Pacific side, or on the lee of the islands, cloud free areas are seen. This is a result of obstruction of fog advection by the islands.

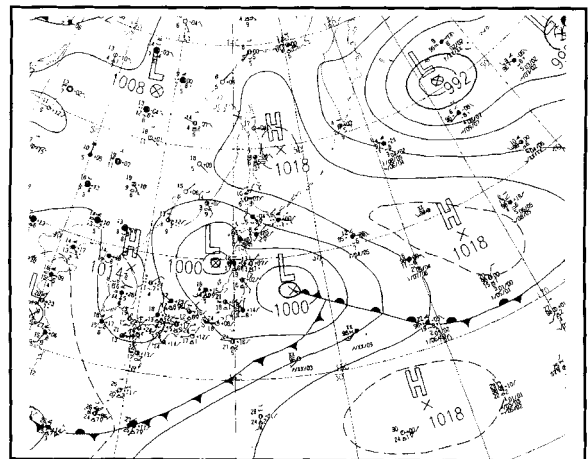
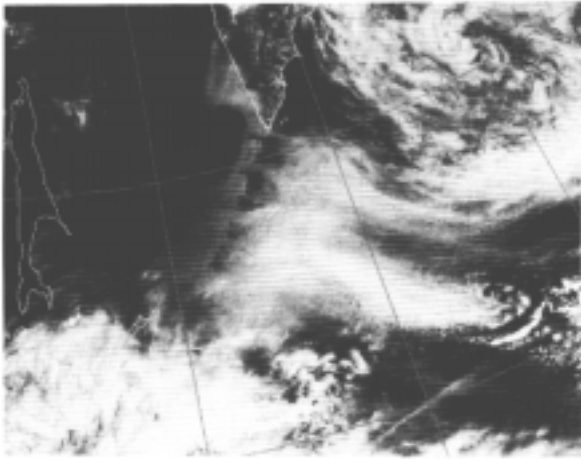


Figure 6-4-2. Sea fog at 00UTC, June 4, 1998.
Left: Visible image. Right: Surface weather chart

(3) Inland fog

Figure 6-4-3 shows an example of occurrence of local fog in the inland in eastern Japan. These fogs occurred by radiation cooling since the middle of the night. In the daytime, the area gradually diminished by the temperature rise due to sunshine. So the fogs had passed the maturity at this time. A somewhat large fog can be identified from around the Biwa Lake to the Bay of Osaka (A), around the Tsuyama Basin (B) and around the Miyoshi Basin (C). Beside these, small fog areas are scattered at Chugoku, Kii and Shikoku Mountains (all marked by D). In the Hita Basin of Kyushu District, a small spot-like fog area (E) can be recognized. On the infrared image at taken at the same time, these fog areas can hardly identified.

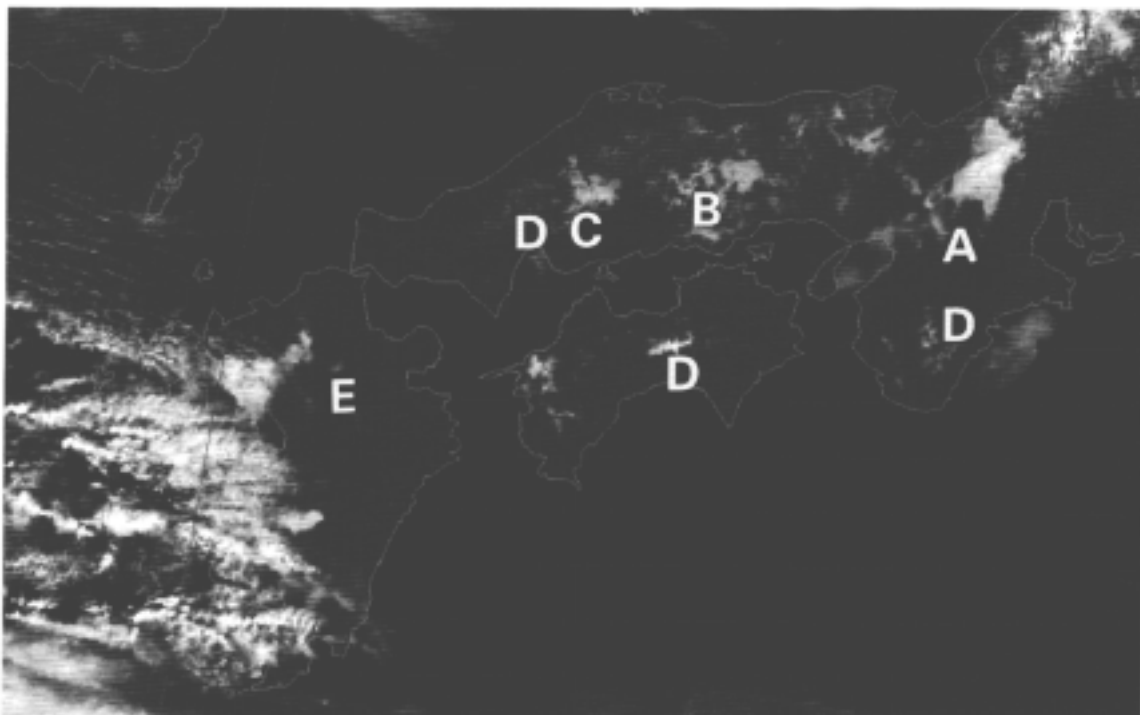


Figure 6-4-3. Inland fog at 01UTC, February 14, 1996. Visible image.
Symbols: Refer to the text.

6.4.2 Low cloud

(1) General features of low cloud

The term “low cloud” in satellite imagery is referred to as Cu, Sc and St as described in Section 2.2. Since these low clouds alone do not bring about serious weather disasters, little attention has been paid to their distinction. But in recent years, identification of low cloud is gathering attention for use in distinction between fair and cloudy in weather forecasting.

The low cloud is seen as a gray or white area on the visible image and as a gray area on the infrared image. On the features of its shape, convective low clouds frequently appear over the sea, and they are seen on the visible image as an widely spread cluster of bunch-like or lump-like cloud cells and on the infrared image as a uniform cloud area with a smooth surface because of the lower space resolution. On the land, stratiform low clouds appear frequently and they are seen as a wide cloud area with a smooth surface on both visible and infrared images. Hasegawa (1998) described that the distinction between Cu and Sc with about the same top height is possible because Cu changes its shape and gray level faster.

(2) Low cloud over the ocean

Figure 6-4-4 shows a low cloud that occurred widely over the ocean. Over the ocean in the winter, such cellular clouds as open cells and closed cells were often observed. Around (O), there are open cells comprised of Cu, and there are active convective clouds of Cb and Cg around (E) northeast of (O). Around (C), there are closed cells, and they were originally striated convective clouds but changed into Sc when the convective activity diminished and the cloud spread out horizontally with the weakening of cold air. This Sc is larger in cloud size than the Cu and Cg clouds in the open-cell region where there is the very cold air.

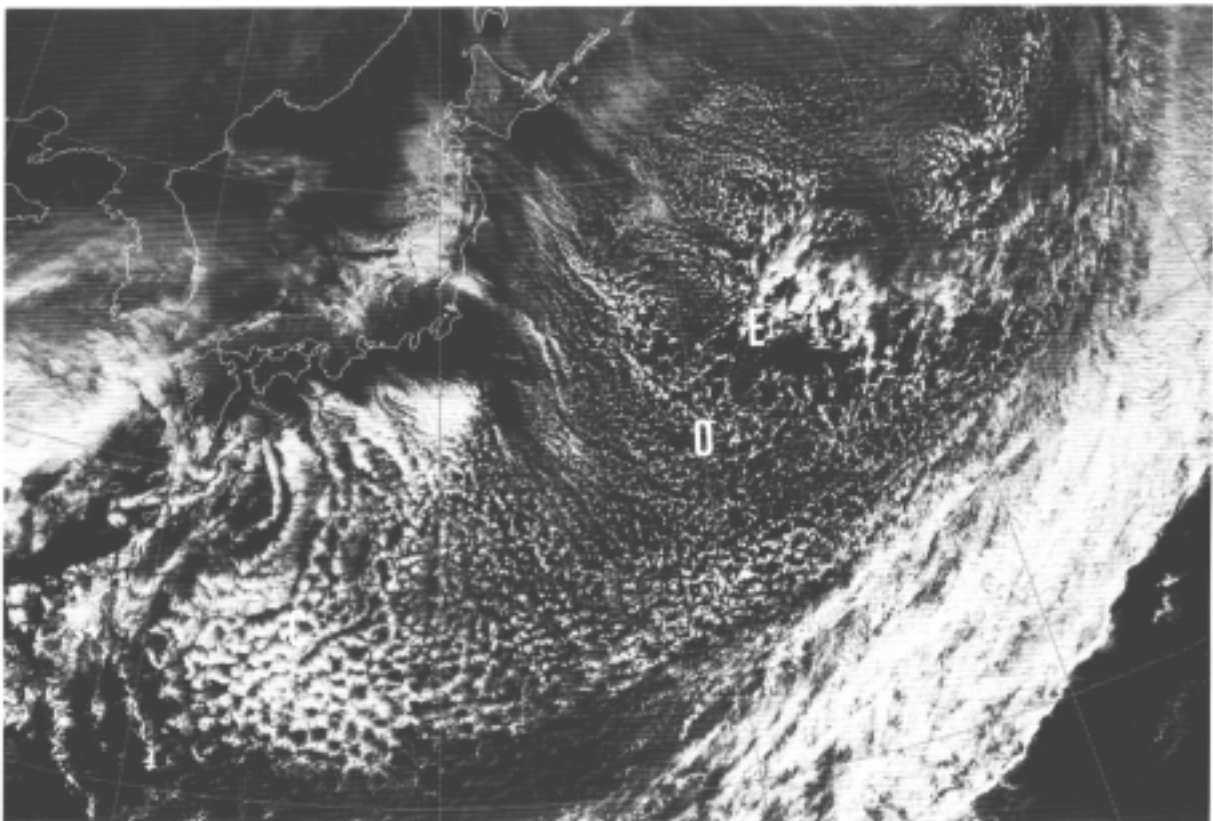


Figure 6-4-4. Low cloud over the ocean at 03UTC, January 23, 1997. Visible image.
For symbols, refer to the text.

(3) Low cloud on the continent

An example of large-scale occurrence of low cloud on the continent is shown in Figure 6-4-5. On the visible image, low cloud (St, Sc) appears in the cloud area widely spreading from a part of northern China to central and southern China. As in this example, the area from central to southern China is frequently covered by low cloud widely from winter to spring. There is an area (A) in southern China, which is whitish in gray scale, and rugged compared with its environs. This is due to the shadow cast from a thin high cloud (see the infrared image) extending from the Indochina Peninsula, and it should be taken notice that this is neither Cu nor other convective cloud.

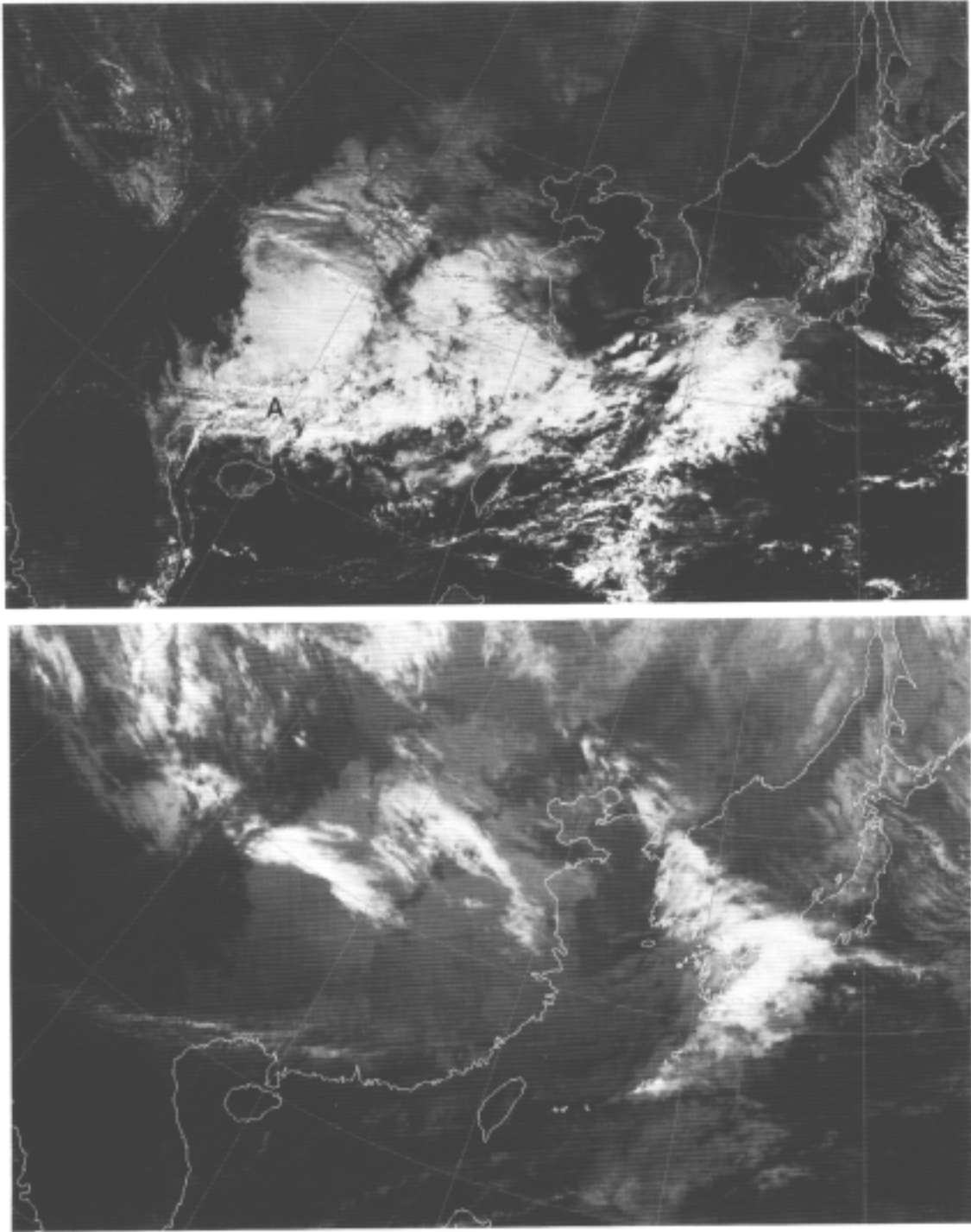


Figure 6-4-5. Low cloud on the continent at 03UTC, February 1, 1998.
Top: Visible image. Bottom: Infrared image.

6.4.3 Characteristic low clouds around Japan

(1) Yamase

Yamase is referred to as a cool and humid east and northeast wind blowing on the Pacific coast of northern Japan from early summer to midsummer. This cool air current is about 1 km in thickness and is accompanied by fog or stratus. It sometimes brings drizzle and prevents sunshine from reaching the surface (Figure 6-4-6 by Urakura, 1995).

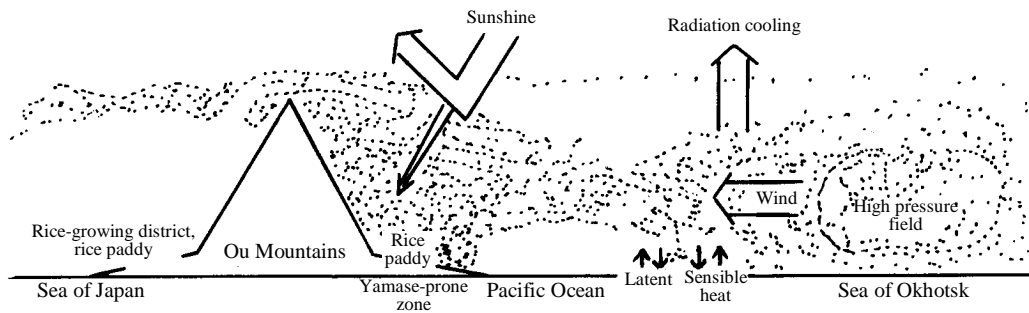


Figure 6-4-6. Conceptual sketch of Yamase. (cited from Urakura, 1995)

In the satellite image, Yamase can be recognized as St or Sc spreading from off Sanriku to the Pacific coast of northern and eastern Japan. In Figure 6-4-7, there is a high with the center in the Sea of Okhotsk and east and northeast winds are blowing out of this high. Due to these winds, the Pacific coast of Hokkaido and Tohoku District is covered by St or Sc, and this is the low cloud associated with Yamase. The low cloud extends from the Pacific coast to the inland of Hokkaido and Tohoku District, however, it is blocked by the mountains and does not extend to the Sea of Japan coast on the lee side (there is an St area off Akita, but it moves north and is in the course of dissipation, so it is different from the low cloud of Yamase). Beside the low cloud of Yamase, another low cloud extends from off Sanriku to the east of Hokkaido (east side of the wedges in the figure). This is St or Sc that occurred due to the cold air behind a low with the center to the east of Japan. Part of it assumes a cellular structure, and it exhibits a different texture from the low cloud of Yamase.

The low cloud of Yamase does not extend over the sea widely and continuously but it is limited to the sea near the shore to the land. This suggests that the low cloud of Yamase was formed near the coast. On the visible image, the cloud area is brighter over the sea than on the land. According to the temperature distribution on the infrared image (Figure 6-4-7) at this time, the top temperature of the low cloud of Yamase is 0 to 3°C, or equivalent to about 1500 m if converted to altitude. Since the cloud top temperature is about the same for clouds over the sea and clouds on the land, the difference in brightness of the low cloud on the visible image may possibly be due to the difference in cloud layer thickness or density of cloud droplets. Therefore, it is thought that the difference in cloud brightness between the sea and land is due to a thicker cloud layer on the land than over the sea because clouds are formed on the land by the topographical ascending current brought about by an easterly wind and the ascending current brought about by surface friction convergence.

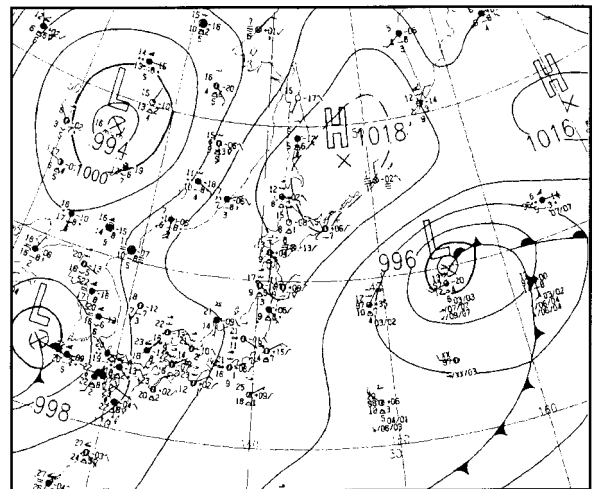
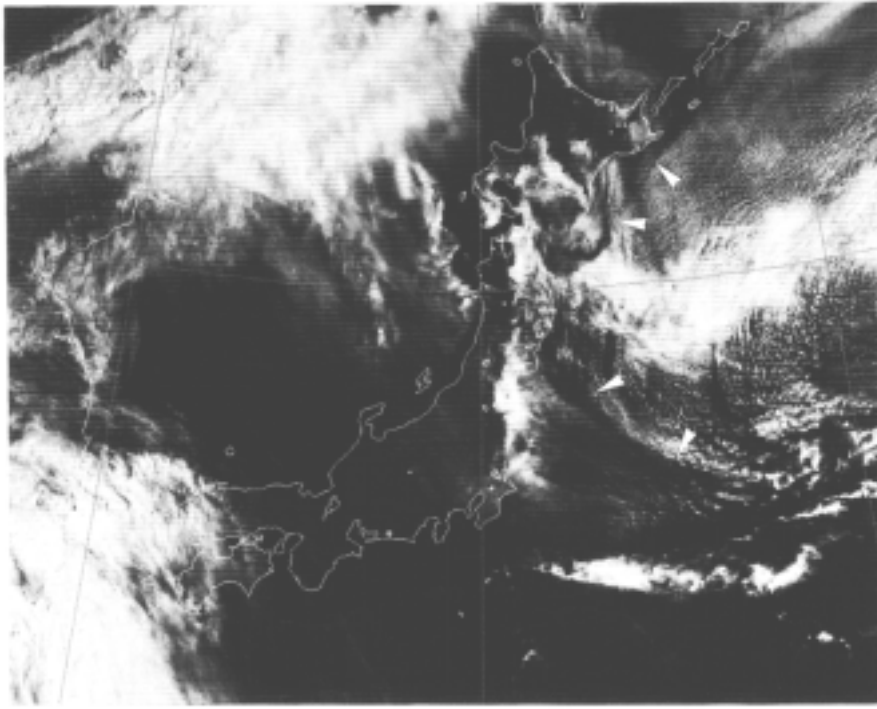


Figure 6-4-7 a.
Surface weather chart at 00UTC, June 8, 1997.



Starting point: 33.50N 138.84E
 End point: 44.75N 150.00E

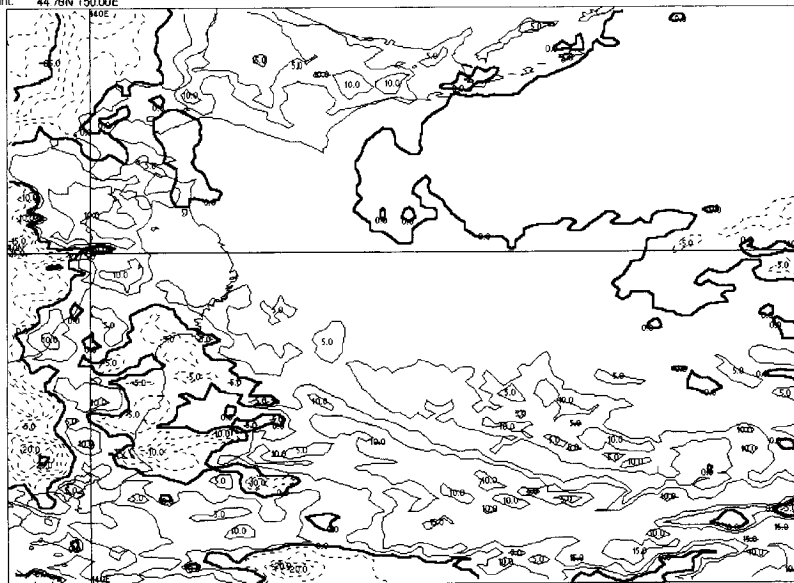


Figure 6-4-7 b. Yamase at 00UTC, June 8, 1997.
 Top: Visible image. For symbols, refer to the text.
 Bottom: Infrared temperature distribution from northern Japan to off Sanriku.
 The isotherm intervals are 5°C, and the bold line indicates the 0°C-isotherm.

(2) Low cloud associated with shear line over the sea south of Kanto

If the hibernal pressure pattern lasts in the cold season, a shear line is formed over the sea south of Kanto District by the current branched at the Chubu Mountains. A characteristic low cloud is formed near this shear line. According to Suzuki and Ando (1992), the trepang and jellyfish types are representative of the cloud area of this sort. Figure 6-4-8 shows a model for this. It is said that the shear line formed by two air current systems coming around the Chubu Mountains closely participates in the formation of these types of cloud area. That is, there are a northeast wind system making a northern detour round the Chubu Mountains and flowing in from the direction of the Sea of Kashima and a west wind system making a southern detour round the Chubu Mountains and flowing in from the direction of the Sea of Enshu. If a shear line is formed over the sea south of Kanto by the currents of these wind systems, a convective cloud occurs along the shear line and the cloud area expands to the north and east of it.

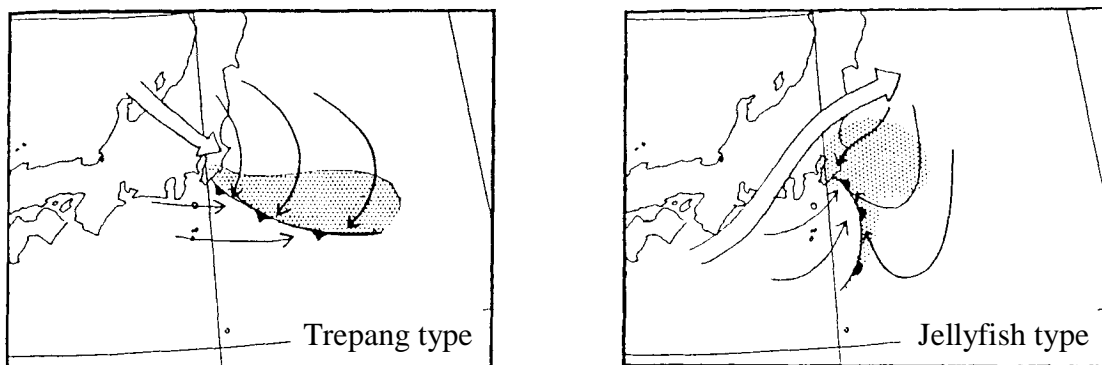


Figure 6-4-8. Model of low cloud associated with shear over the sea south of Kanto (trepang and jellyfish types).
Cited from Suzuki and Ando (1992).
Shaded area: Cloud area. Arrow with thin shaft: Surface wind.
Thick white arrow: Wind above the stable layer.
The shear line is indicated by a front symbol.

The cloud area of the trepang type is comprised of a convective cloud of such a form that the major axis of the cloud area extends in a east-west direction and the southern edge is convex to the south. This cloud area tends to move east and has little effect on the land. In Figure 6-4-9, the low cloud area (N) extending from the Boso Peninsula to the offing southeast of it is a cloud area of the trepang type. A cloud comprised of Cu extends along the southern edge from off the Izu Peninsula in an east-southeast direction, and a cloud comprised of Sc spreads on the north. The trepang type seldom brings foul weather on the land because precipitation tends to be limited to the Cu line on the southern edge, the cloud area only covers the Boso Peninsula by its western tip, and the cloud area moves in a direction away from the land.

A cloud area of the jellyfish type forms a pattern that resembles a comma with the major axis of the cloud area extending in a south-north direction and a concave southwest edge and a convex northern edge. The cloud area is comprised of low clouds, in particular, of Cu on the south and east sides in many cases. When the cloud area develops, the north side assumes a multi-layer structure in which high and middle clouds cover the low cloud. This cloud area tends to move north, and it affects Kanto District. In Figure 6-4-10, the cloud area (K) lying over the sea south of Boso Peninsula is a cloud area of the jellyfish type. The convective cloud line (Cu, marked by wedges in the figure) corresponding to a leg of a jellyfish extends north to south and the cloud area

on the north side (Cu or Sc) corresponding to the head of a jellyfish moves north while it expands. The jellyfish type is apt to bring foul weather on the land because precipitation is observed in a wide area within the cloud area, the cloud area moves in a direction toward the land, and it develops as a low if it is connected with an upper trough.

A cloud area of the trepang type may transform itself into the jellyfish type by the approach of an upper trough (there is no reverse transformation). Therefore, it is necessary for forecasting to watch pattern alterations on the satellite image.

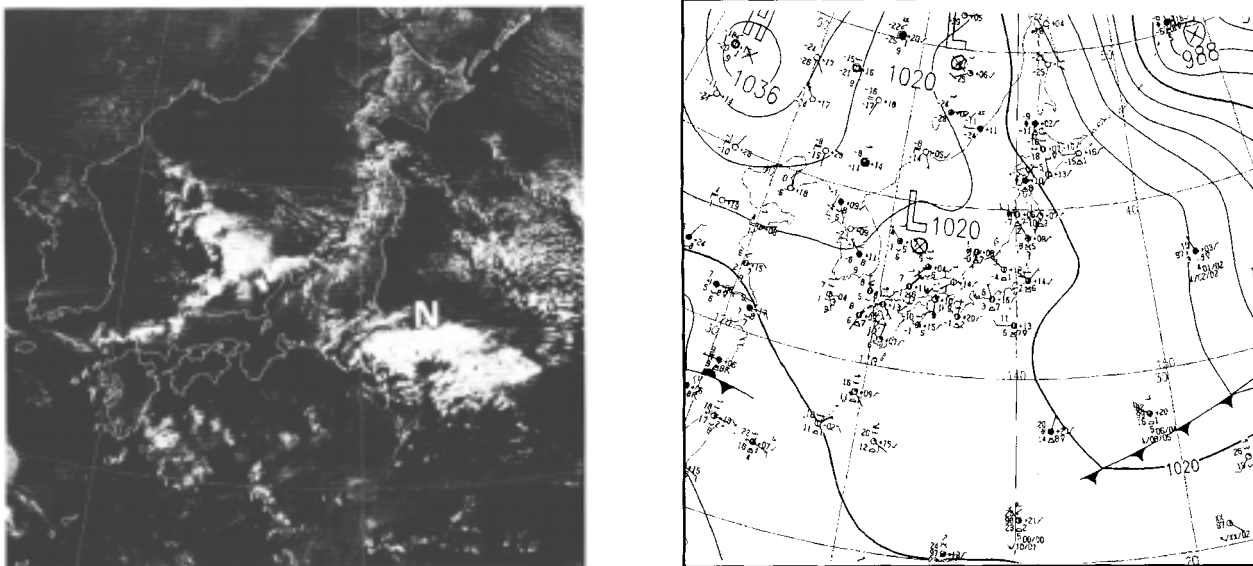


Figure 6-4-9. Low cloud associated with shear over the sea south of Kanto (trepang type: February 16, 1998). Left: Visible image (at 03UTC). Right: Surface weather chart (at 00UTC).

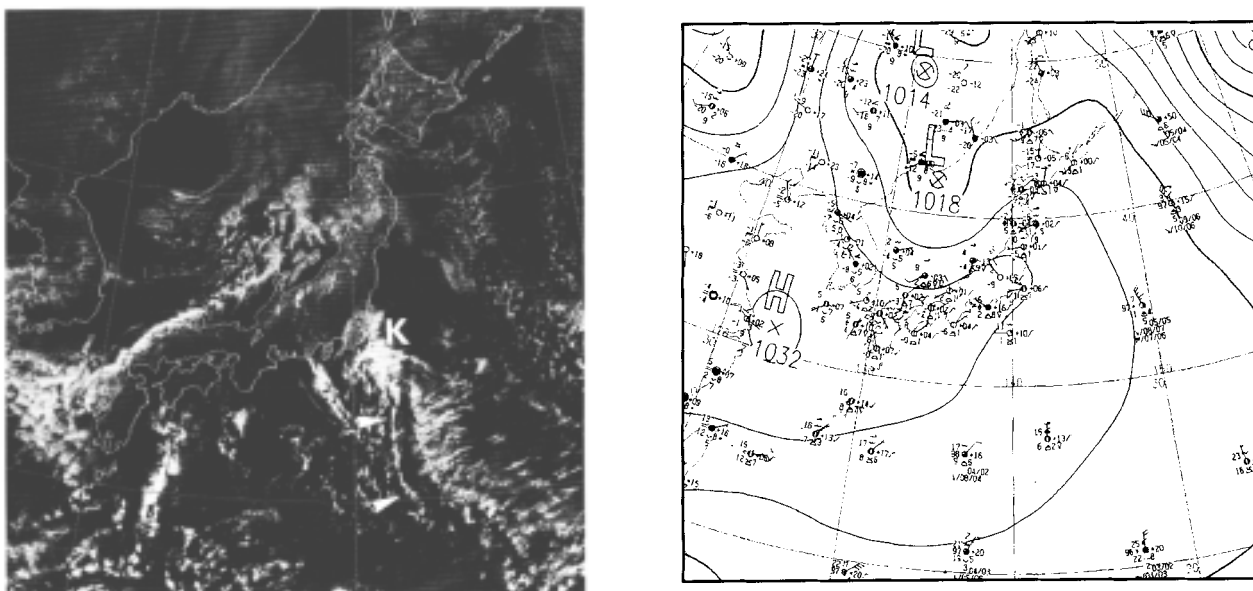


Figure 6-4-10. Low cloud associated with shear over the sea south of Kanto (jellyfish type: January 30, 1998). Left: Visible image (at 03UTC). Right: Surface weather chart (at 00UTC).

(3) Coastal front

The coastal front is a local front formed between a relatively warm and humid air mass blowing from the sea and a cold air mass created on the land. It appears on the Pacific coast from eastern to western Japan, and it involves rain, wind shear, visibility hindrance and other types of foul weather. A model was devised (Figure 6-4-11, Forecast Division of the Meteorological Agency et al., 1993). According to the model, a low cloud is formed by an air mass upgliding over stagnant cold air near the ground surface. On the satellite image, a coastal front can be recognized as a low cloud area captured by the topography. Because the coastal front appears away from fronts, lows and other synoptic-scale disturbances, its watching is important from the viewpoint of forecasting.

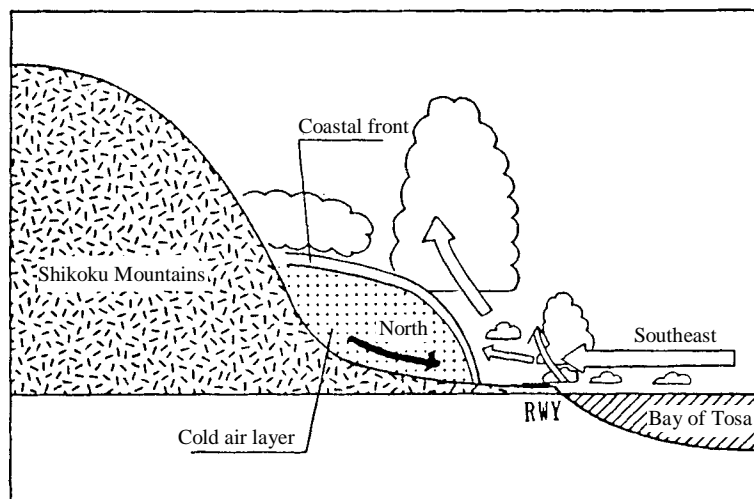


Figure 6-4-11. Model for coastal front at Kochi (cited from the Forecast Division of the Meteorological Agency et al., 1993).

Figure 6-4-12 shows an example of occurrence of a coastal front in eastern Japan. The low still lies over the East China Sea, and the Ci cloud at the tip of the cloud area associated with the warm front extends to Shikoku and Chugoku Districts. Aside from these cloud areas associated with synoptic-scale disturbances, a low cloud area (marked by wedges) spreads over Kanto District, and this is a coastal front seen on the satellite image (another low cloud spreads over Tokai District and its offing, but its cause is thought to be different because of its different movements from the one over Kanto District). The low cloud area was formed when a cold air layer was formed in the Kanto Plain and near the ground surface and a southern current upglided over this cold air layer. From the upper-air observation (not shown) at Tateno, the thickness of the cold air layer represented by an east or northeast wind can be estimated at 500 to 1000 m. According to the measurement from the satellite, the top temperature of the low cloud is 0 to 5°C, which is equivalent to a top height of 1500 to 2000 m. The low cloud of Kanto District is almost limited to the land, reflecting the structure of a coastal front, which is formed by upgliding over stagnant cold air on the ground surface.

The coastal front is observed in western Japan as well (Figure 6-4-13). Since western Japan has few plains of such vastness as to foster cold air and let it stagnate as in the Kanto Plain, the scale of a low cloud area associated with a coastal front is smaller than in eastern Japan. In this example, the low cloud areas (marked by wedges) seen in the Kii Peninsula and Shikoku District are formed by a coastal front. Each exists in a small plain spreading on the south of the mountains. There is

a low in the East China Sea and a warm front accompanies the low. The cloud area extending from this warm front extends to Kyushu District. However, the low cloud area described here is different from such a synoptic-scale cloud area. From the upper-air observation at Shionomisaki (not shown), the thickness of the cold air layer represented by an easterly wind can be estimated at about 500 m. According to the measurement from the satellite, the top temperature of the low cloud is around -5°C , which is equivalent to a top height of about 2000 m.

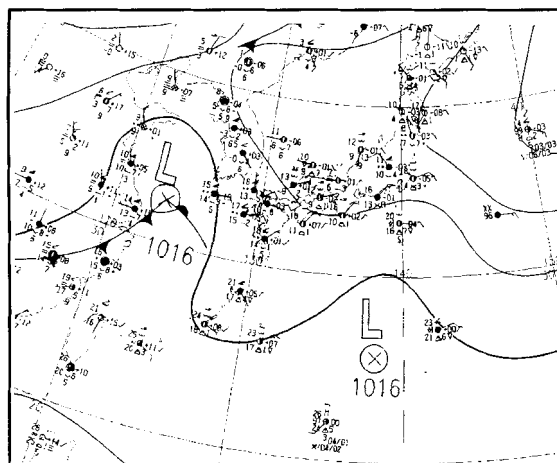
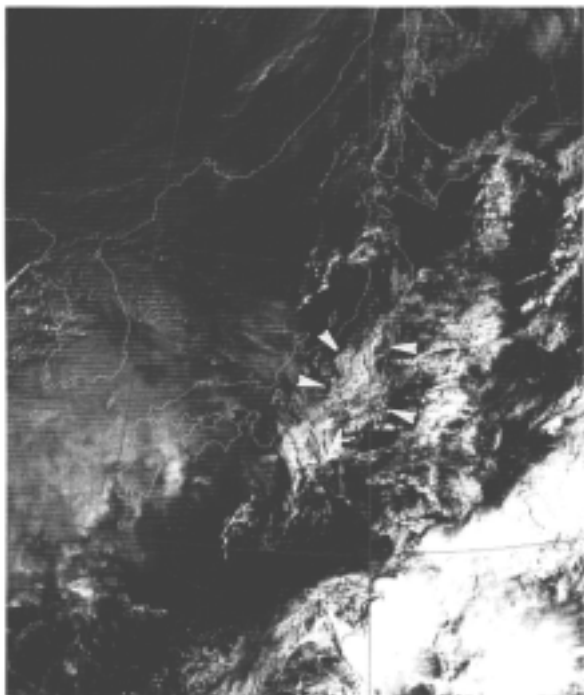


Figure 6-4-12. Coastal front in eastern Japan at 00UTC, November 21, 1997.
 Left: Visible image. Wedges indicate a low cloud area associated with a coastal front.
 Right: Surface weather chart.

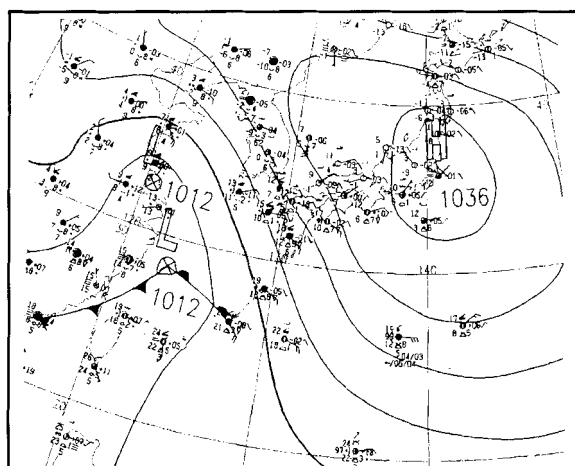
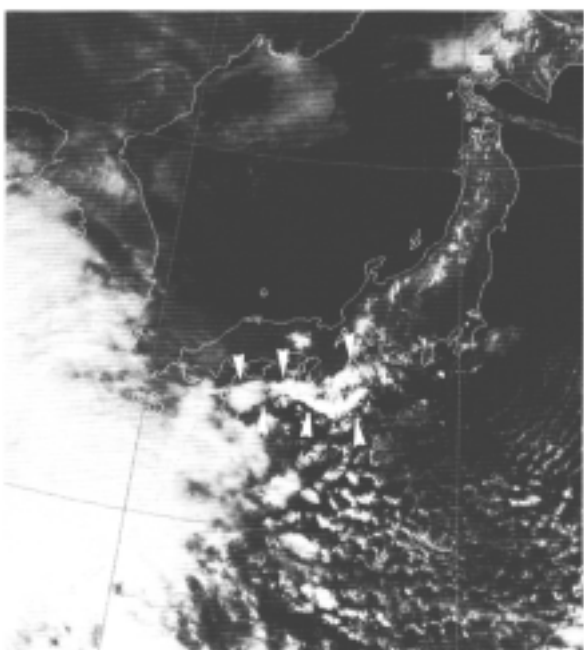


Figure 6-4-13. Coastal front in western Japan on February 19, 1998.
 Left: Visible image (at 03UTC). Wedges indicate low cloud areas associated with coastal front.
 Right: Surface weather chart (at 00UTC).

(4) Barrage cloud associated with foehn

If a moist air mass rises along a slope of a mountain, the air mass becomes saturated and produces a cloud on the windward side of the mountain. When it blows down on the lee side, it dries by an adiabatic warming and the cloud dissipates (Figure 6-4-14). This phenomenon is called foehn. On the satellite image, a cloud occurs on the mountain slope on the windward side, and the weather is fair on the lee side. The low cloud occurring associated with foehn on the windward side is called barrage cloud (Bader et al., 1995).

In Figure 6-4-15, south or southwest strong winds blow toward the lows in Sakhalin and the Korean Peninsula and they prevail over the Japanese Islands. Around Japan, a moist air current flows in from the sea to the south. By forced ascending along a slope, low clouds comprised chiefly of Cu are formed on southern or southwestern slopes in the Chubu Mountains, Kii Peninsula and Kansai and Shikoku Districts. If observed on the animation images, it can be ascertained that these clouds are checked by mountains or other obstacles and are stationary. Hence the name barrage cloud. The weather was fair in the Hokuriku and Setouchi Districts where a dry air mass coming over the mountains blows down, and the maximum temperature exceeded 30 degrees at Niigata and Kanazawa by the foehn.

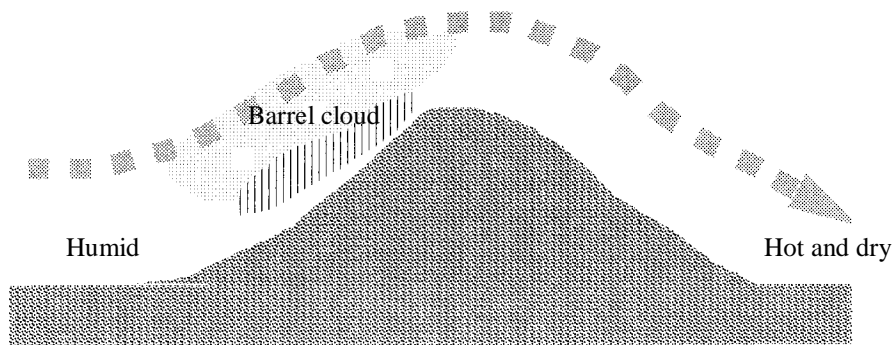


Figure 6-4-14. Schematic of foehn

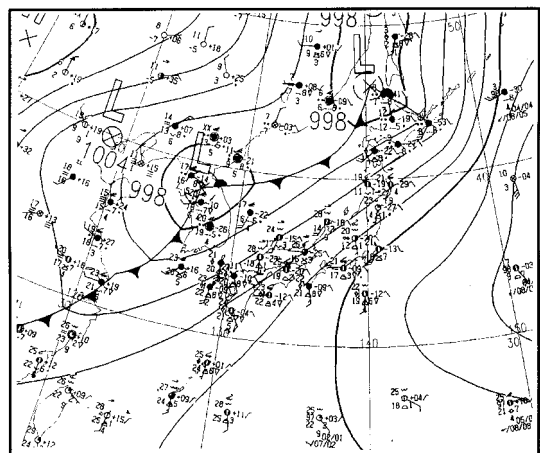
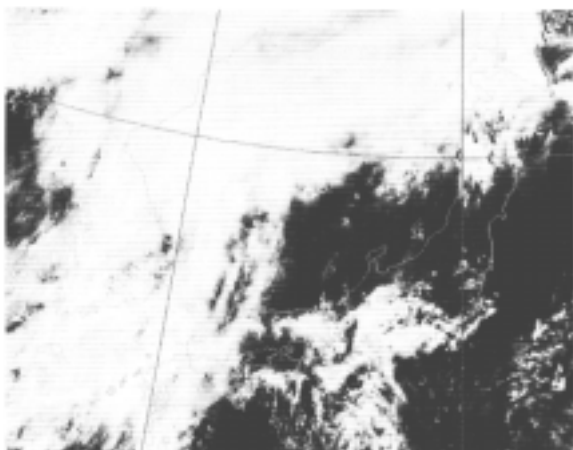


Figure 6-4-15. Barrage cloud associated with foehn on May 2, 1998. Left: Visible image (at 03UTC). Right: Surface weather chart (at 00UTC).